

Title: The impact of submarine copper mine tailing disposal from the 1970s on Repparfjorden, northern Norway

Beata Sternal^{a,b,*}, Juho Junttila^a, Kari Skirbekk^a, Matthias Forwick^a, JoLynn Carroll^{a,c}, Kristine Bondo Pedersen^c

a) Department of Geosciences, UiT The Arctic University of Norway in Tromsø, Dramsveien 201, 9037 Tromsø, Norway

b) Institute of Geology, Adam Mickiewicz University in Poznań, Bogumiła Krygowskiego 12, 61-680 Poznań, Poland

c) Akvaplan-niva, Fram Centre - High North Research Centre for Climate and the Environment, 9296 Tromsø, Norway

* corresponding author: beata.sternal@uit.no, sternal@amu.edu.pl

Abstract:

We investigate the state of sedimentological environment and contaminant status of Repparfjorden (N Norway) impacted by submarine disposal of mine tailings during the 1970's. Based on examination of the sedimentological and geochemical properties of seventeen sediment cores, the impact of tailings disposal is mainly restricted to the inner fjord where the discharge occurred. Sediment cores retrieved from the inner fjord contain layers of mine tailings up to 9-cm thick, 3-9 cm below the seafloor. Spreading of the tailing-related metal Cu and particles is limited to the inner fjord and to a 2 cm layer in one core from the outer fjord. Two interrelated factors, fjord morphology and sedimentation rate, controlled the distribution of contaminant-laden tailings in the fjord. The mobility of Cu from buried contaminated sediments to the sediment-water interface in the inner fjord indicates that benthic communities have been continuously exposed to elevated Cu concentrations for nearly four decades.

Keywords: fjord; submarine mine tailing disposal; contaminated sediments; grain-size distribution; heavy metals; sedimentation rate

1. Introduction

Coastal zones are of great ecological, economic and social importance (Martínez et al., 2007) and with increasing human activities they are particularly prone to anthropogenic pollution. Especially vulnerable are estuaries, forming a natural sink for (contaminated) sediments, that due to their dynamic regime may also act as sources of sediments, both seaward and up-estuary (Ridgway and Shimmield, 2002). There are different types of marine contaminants, originating from e.g. sewage effluents, agricultural run-offs, industrial effluents, oil spills, litter, etc. (e.g. Islam and Tanaka, 2004). Among them, although more marginal in a global scale, are mine tailings.

Mine tailings are a waste product resulting from the mechanical and chemical separation of minerals from geological material retrieved during mining. They contain a mixture of milled ore (often of high residual metal concentrations), water and sometimes process chemicals. The most common way of disposing and storing mine tailings is on-land (up to 99%) but an alternative, marine disposal, is practiced in Norway and Papua New Guinea, and at some locations in Turkey, England, Greece, France, Chile and Indonesia (Vogt, 2013). Marine tailings disposal approaches are differentiated based mainly on the depth of tailings discharge, an important factor from the perspective of potential ecological and environmental impacts (for review see e.g. Ramirez-Llodra et al. 2015). However, recent legal frameworks limit all types of marine disposal with exceptions under specific conditions, as for example described within the London Protocol (IMO, 2016), a globally leading initiative to protect marine environment.

Post-discharge studies of historical submarine tailings disposal operations have identified impacts on the environment. They are primarily confined to the area of the disposal and may include physical and geochemical alteration of the bottom sediment, smothering of benthic organisms, reduction of marine biodiversity, risk of bioaccumulation of heavy metals in aquatic organisms (e.g. Burd, 2002; Elberling et al., 2003; Hughes et al., 2015; Josefson et al., 2008; Larsen et al., 2001; for review see also Ramirez-Llodra et al., 2015). Even though operators are required to establish practices to minimize the potential environmental consequences, some of the documented historical disposal activities have impacted a wider area than expected (e.g. Edinger, 2012; Perner et al., 2010).

Submarine tailings discharge has been carried out in Norwegian fjords for more than 100 years. There are at least 26 historical sites where relatively large discharges and/or discharges with the release of potentially toxic metals have occurred (Kvassnes and Iversen, 2013). However, as underlined by Ramirez-Llodra et al. (2015), there are no reports providing information on the exact composition of discharges, i.e. neither detailed chemistry and their changes, nor the

1 fate of these materials once they enter the marine environment. This gap of knowledge is of particular significance since
2 fjords are estuaries with characteristic morphological features, circulation and stratification patterns. The presence of
3 basin(s) separated by sill(s) make them depocenters for (contaminated) sediments, thus rendering them particularly
4 susceptible to pollution impacts.

5 Various analytical tools are used to map the historical contaminations of the marine environment (e.g. estuaries)
6 recorded in sediments (e.g. Ridgway and Shimmiel, 2002). However, the choice of applied techniques strongly
7 depends on the type of pollutants. The disposed mine tailings comprise large quantities of processed geological
8 material, usually enriched in concentrations of extracted metal(s). Therefore, the basic method used include analyzing
9 multi-element geochemistry (e.g. Edinger et al., 2007; Elberling et al., 2003; Larsen et al., 2001; Little et al., 2015;
10 Odhiambo et al., 1996; Perner et al., 2010), often supplemented by analyses of organic carbon content and grain-size
11 distribution, both being closely interrelated with most of the investigated elements/metals (Elberling et al., 2003;
12 Edinger et al., 2007; Little et al., 2015). They are occasionally supported by radionuclide activity measurements to
13 provide an independent time scale (e.g. Elberling et al., 2003; Odhiambo et al., 1996; Little et al., 2015; Perner et al.,
14 2010). In a perspective of the processes governing the spreading and potential impacts of the discharged mine tailings
15 on the marine environment it seems equally important to track the distribution of the tailing particles themselves, and
16 not only the tailing-related contaminants. Grain-size analysis may provide additional evidence to understand material
17 dispersion pattern, as exemplified by Okada et al. (2009) in their research on the spatial distribution of dredged material
18 disposed in UK coastal waters.

19 The main aim of this study is to assess the state of the sedimentological environment and the potential impacts of
20 submarine tailings disposal from copper (Cu) mine activities on the fjord Repparfjorden (northern Norway), nearly 40
21 years after its cessation. The fjord has two basins, the inner and outer basin separated by a sill. Mine tailings were
22 discharged into the inner part of the fjord during copper mining operations in the 1970s in an amount estimated at ~1
23 million tons (Kvassnes and Iversen 2013).

24 Previous investigations of Repparfjorden are sparse and only reported in grey literature and in consultancy reports
25 (Christensen et al., 2011; Dahl-Hansen and Velvin, 2008). These authors mainly examine surface sediment samples,
26 characterizing primarily the present state of the Repparfjorden environment. They document elevated concentrations of
27 heavy metals in surface sediments in the vicinity of the discharge point, while finding no significant differences
28 between the inner and outer fjord in benthic organisms or in benthic biodiversity. In addition, one ²¹⁰Pb-dated core
29 collected from the central part of the fjord (Fig. 1) was investigated for heavy metal concentrations revealing that only
30 pollution of a negligible level occurred in surface sediments (Christensen et al., 2011). The characteristics of the tailings
31 discharged during the 1970's were partly a focus of Pedersen et al. (2016) in terms of metal availability and its potential
32 mobilization. In their study, a 10-cm-thick sediment sample taken 5 cm below the seafloor from the inner fjord was
33 investigated, assuming to be representative of the mine tailings. Chemical analyses revealed a relatively high Cu
34 concentration that was associated with more available fractions.

35 Here we examine the sedimentological and geochemical records obtained from seventeen short sediment cores retrieved
36 from the entire fjord. We give particular attention to the reconstruction of sedimentation based on grain-size
37 characteristics and sediment accumulation rates, as well as potential sediment transport paths with prime focus on
38 lateral and vertical spreading of mine-tailing related contaminants (metals) and particles. In light of the obtained results,
39 we also address questions of potential long-term impacts of environmental pollution in the fjord.
40

41 2. Study area

42 Repparfjorden, located in Finnmark County (northern Norway) is an approximately 13 km long, up to 4 km wide and c.
43 37 km² large fjord (Fig. 1). Water exchange with the open ocean occurs through Kvalsundet and Sammelsundet. The
44 fjord comprises two main basins, a smaller basin with maximum water depth of c. 65 m in the inner fjord and a larger
45 basin with up to c. 120 m depth of the outer fjord. They are separated by an E-W orientated sill of approximately 50 m
46 depth. An additional sill, interpreted to be part of an end moraine (Marthinussen, 1960) crosses the fjord mouth.
47 Repparfjorden is a temperate non-glaciated river-influenced fjord, with the main river Repparfjordelva at the fjord head.
48 This river drains an area of 1019 km². A delta and a tidal flat occur at the transition from the river to the fjord.
49

50 Copper deposits of the Ulveryggen and Nussir ore formations occur south of Repparfjorden. They are associated with
51 the Repparfjord Tectonic Window within the Caledonides. The first mining activities of Repparfjorden ore deposits
52 commenced in the beginning of the 20th century, however, large-scale operations started in the 1970s. Between 1972
53 and 1978 (1979) approximately 3 Mt of ore were mined from open pits in the Ulveryggen formation (Sandstad et al.,
54 2012) and approximately 1 million tons of tailings were subsequently discharged at the inner fjord bottom (Kvassnes
55 and Iversen, 2013). The exact composition of the tailings before disposal (particle size, geochemical characterization
56 and chemicals used) along with the location of the discharge outlet are uncertain and the information provided below
57 are based on disparate sources, namely brochures issued by the mining company in the 1970s and community
58 interviews (Svendsen J., pers. comm.). The mine tailings were discharged about 1.5 km out from the processing plant
59 through a pipeline at a depth of about 60 m (for location see Fig. 1C). The pipeline, suspended 20 m above the seafloor,
60 had openings at its outlet over a length of 600 m spaced at intervals of 100 m. About 80% of the ore was milled to the
61
62
63
64
65

1 size of 74 μm , subjected to the flotation process and thereafter mixed with flocculent chemical and disposed at the fjord
2 bottom. The flocculent (likely Separan NP10) was used to prevent mobilization and facilitate rapid settling of the tailing
3 particles. According to recently conducted chemical characterization of tailings from the Ulveryggen deposits, that were
4 produced using similar methods as in the 1970s, the Cu concentrations varies between 707 and 1090 mg/kg depending
5 on the grain-size fraction of analyzed subsamples (Kleiv, 2011).

6 **3. Material and methods**

7 **3.1. Sampling procedure**

8 The material for this study was collected during two cruises in April 2013 and June 2015 with R/V Helmer Hanssen of
9 UiT The Arctic University of Norway in Tromsø (UiT). Sediment cores, up to 21 cm long, were taken from seventeen
10 stations covering the entire fjord (Fig. 1, Table 1). They were retrieved with a multi corer (MC) or with a box corer
11 (BC), respectively. The MC contains six plastic liners (up to 80 cm long; 11 cm outer diameter), whereas BC consists of
12 a metal box with dimensions of 50 cm \times 50 cm \times 50 cm into which plastic liners were pushed to sub-sample individual
13 sediment cores. The surfaces of all of the cores analyzed in this study were undisturbed. Whenever possible a duplicate
14 of each core was retrieved to ensure enough amount of (dry) material for the purpose of this study (~40 g) as well as for
15 the foraminifera analysis (preferable >100 g) (Skirbekk et al., in prep.) and detailed chemical analyses (~30 g)
16 (Pedersen et al., sub.). The seventeen cores together with one of their duplicates were sliced into samples of 1-cm
17 thickness and frozen immediately after retrieval. All samples were freeze-dried prior to the analyses (for an overview of
18 analyses see Table 1). Unless otherwise stated, each core together with its duplicate will be referred by a short name
19 according to the following pattern, e.g. HH13-001-MC-MF-D, hereafter named 001, and IG15-1-1039-BCA, hereafter
20 named 1039, etc.

21 **3.2. Sedimentological properties**

22 Grain-size analyses were performed on all samples at the Department of Geosciences at UiT (Table 1). The sub-samples
23 (2 g) pre-treatment followed the procedures described by Dijkstra et al. (2016). The grain-size measurements were
24 carried out with a Laser Diffraction Particle Size Analyzer (Beckman Coulter LS 13 320) with Polarisation Intensity
25 Differential Scattering (PIDS) analyzing the range from 0.017 to 2000 μm . The measurements were performed in three
26 runs of 60 seconds and the average was calculated subsequently. Sediments classification is according to Folk's (1954)
27 scheme, whereas grain-size statistical parameters were calculated with the GRADISTAT software (Blott and Pye, 2001)
28 applying the geometric method of moments.

29 **3.3. Sediment geochemistry**

30 Heavy metal concentrations were determined for all pulverized sediment sub-samples (2 g) of fractions <2 mm (Table
31 1). Measurements of As, Ba, Cd, Co, Cr, Cu, Ni, Pb, Ti, V and Zn concentrations in samples from 14 cores were
32 conducted at Unilab Analyse AS via the sub-contracted ALS Laboratory Group Norway AS, using a inductively
33 coupled plasma atomic emission spectrometer (ICP-AES) or inductively coupled plasma sector field spectrometer (ICP-
34 SFMS) following nitric acid digestion. Mercury concentrations were determined using atomic fluorescence
35 spectrometer (AFS). In both cases, standard procedures following Norwegian Standard 4770 and 4768 were applied
36 (Norwegian Standard 1994, 1989, respectively). Metal concentrations of As, Ba, Cd, Co, Cr, Cu, Ni, Pb, V and Zn in
37 samples from 3 cores were analysed at the Technical University of Denmark (DTU), also based on acid digestion and
38 using inductively coupled plasma – optical emission spectrometry (ICP-OES) following Norwegian Standard 4770
39 (Norwegian Standard 1994).

40 Total organic carbon (TOC) was measured in bulk sediments for all sub-samples (2 g) at UiT and at DTU (Table 1).
41 The TOC content was calculated accordingly $\text{TOC} = \text{TC} - \text{TIC}$, where TC is total carbon and TIC is total inorganic
42 carbon content. At both laboratories, TC was measured using a LECO CS-200 instrument. At UiT, the content of TIC
43 was measured using the LECO CS-200 instrument after removing calcium carbonates from the samples with ~20%
44 HCl. At DTU, TIC measurements were carried out in a Scheibler apparatus after dissolving calcium carbonates with
45 ~10% HCl.

46 **3.4. Sediment accumulation rates**

47 The assessment of modern sediment accumulation rates (SARs) was based on the interpretation of ^{210}Pb and ^{137}Cs
48 activity profiles of eight cores retrieved from both the inner and outer fjord (Fig. 1, Table 1). The activities were
49 measured by gamma spectroscopy using a high-purity germanium detector (Canberra GX2520) at the Institute of
50 Geology, Adam Mickiewicz University in Poznań (Poland) following procedures described by Szczuciński et al.
51 (2013). Each freeze-dried sub-sample (up to 30 g) was homogenized and packed in a plastic sealed container, thereafter
52 stored for several weeks. To enable the calculations of SARs excess ^{210}Pb activities ($^{210}\text{Pb}_{\text{ex}}$) were determined by
53 subtracting the ^{210}Pb supported activity ($^{210}\text{Pb}_{\text{supp}}$) (average of ^{214}Pb , ^{214}Bi and ^{226}Ra) from the total ^{210}Pb activity
54 ($^{210}\text{Pb}_{\text{tot}}$).

To calculate SARs the Constant Initial Concentration model was used (for review see e.g. Carroll and Lerche, 2003) assuming that the $^{210}\text{Pb}_{\text{ex}}$ concentration in surface sediments is constant over time and the $^{210}\text{Pb}_{\text{ex}}$ flux to the surface of the sediments together with the accumulation rate are proportionally variable. The assumption of a closed system in this model imposes that the $^{210}\text{Pb}_{\text{ex}}$ activity profile shall decrease exponentially with depth. However, non-steady sedimentation caused by mine tailing discharge during the 1970s and sediment surface mixing are probably the main reason for non-exponential down-core decreases of $^{210}\text{Pb}_{\text{ex}}$ activity with depth (for details see section 4.3). In consequence, $^{210}\text{Pb}_{\text{ex}}$ activity profiles were divided into intervals representing different accumulation rates and then the average SAR for each interval was calculated, following the equation:

$$\text{SAR} = \lambda \times z \times (\ln A_0/A_z)^{-1}$$

where λ is ^{210}Pb disintegration constant ($=0.03118 \text{ yr}^{-1}$), z is a depth in a core (cm) (in this case thickness of the interval), A_0 is the $^{210}\text{Pb}_{\text{ex}}$ concentration at the surface (top layer of the interval), and A_z is the $^{210}\text{Pb}_{\text{ex}}$ concentration at depth z (bottom layer of the interval). To validate our ^{210}Pb -derived assessment of SARs we used anthropologically induced ^{137}Cs as a time marker with its first occurrence during the early 1950s and maximum activity around 1961 (e.g. Robbins and Edgington, 1975). Due to limitations in the use of this dating method (e.g. non-steady sedimentation and sediment mixing) calculated SARs should be treated as approximate SARs.

3.5. Background heavy metal concentrations

In order to assess the degree of heavy metal pollution for Repparfjorden sediments containing discharged mine tailings, it is important to first distinguish between natural (background) and anthropogenic metal loads. The natural variation in heavy metals is mainly attributed to variations in sediment grain-size, hence also their mineralogical composition. In general, heavy metals have an affinity for finer sediment fractions (e.g. Barbanti and Bothner, 1993; Brook and Moore, 1988; Zonta et al., 1994). Accordingly, the simplest and highly recommended approach to assess the natural local background levels is to determine heavy metal concentrations in texturally equivalent subsurface sediment core samples obtained from a depth below any possible contamination or biological mixing (Loring and Rantala, 1992). To meet the “pristine” criterion in this study a twofold approach was applied. Firstly, the sediments were confirmed as being deposited before tailings disposal. We identified core sections deposited before the year 1970 using our derived SARs. These sections were inspected for heavy metal concentrations to identify the lowest concentrations, considered to reflect the least impacted levels. Using this procedure, four cores were chosen: 002, 003, 005 and 1075. In order to fulfil the second condition of textural equivalence three background metal levels are proposed. They were determined by averaging the three lowest concentrations of a specific heavy metal found in the four chosen cores in an equivalent textural sediment group, namely of comparable mud content (Table 2).

To validate our estimations, we compared obtained background levels with available geochemical data from Repparfjorden (Christensen et al., 2011) (Fig. 1). According to Christensen et al. (2011) the lowest measured concentrations for Cd, Cu, Pb and Zn were found in the deepest sample (14-15 cm) consisting of 73% mud and ^{210}Pb -dated to the year 1939. The concentrations (Table 2) are of comparable values with our background level 1, estimated for samples composed of 66% mud on average.

The major portion of sediments in temperate fjords, like Repparfjorden, derives from fluvial sources (Syvitski et al., 1987). Therefore, in the assessment of natural heavy metal concentrations it is also crucial to consider the natural chemical composition of sediments from the Repparfjordelva catchment. For this purpose, we used the chemical composition of overbank sediments (floodplain sediments) (Ottesen et al., 2000), since they are regarded the most representative for geochemistry of the drainage area (Ottesen et al., 1989). As presented in Table 2, the metal concentrations in overbank sediments (Ottesen et al., 2000) are one order of magnitude higher in some cases compared to the samples presented in this study. This is likely due to the usage of different sediment fractions. The metal concentrations in overbank sediments were analyzed in the mud fraction ($<63 \mu\text{m}$), whereas in our study concentrations were measured in a gravel-free fraction ($<2 \text{ mm}$). However, if we recalculate proportionally the percentage content of mud fraction to account for grain-size variations, our estimates are more comparable to the concentrations of overbank sediments.

3.6. Geoaccumulation index

The degree of heavy metal contamination of the sediments was assessed using the geoaccumulation index (I_{geo}) proposed by Müller (1969) and defined as:

$$I_{\text{geo}} = \log_2 (C_n/1.5B_n)$$

where C_n is a measured concentration of a given metal in sediment layer X , B_n represents background concentration of a given metal either found in the literature or measured in texturally equivalent uncontaminated sediments. To meet the criterion of textural equivalence, the established background levels (see section 3.5 and Table 3) are a function of the mud content in the sediment sample for which the index was calculated. A factor of 1.5 is introduced to account for possible variations in background values. The level of contamination is subsequently based on increasing values of

calculated I_{geo} and presented as seven descriptive classes with the highest class representing 100-fold enrichment above background values (Table 3).

3.7. Statistical analysis

Pearson correlation was calculated for standardized data using the Past 3.06 software. The transformation applied for samples of each core separately brings all values to compatible units of a distribution with a mean of 0 and a standard deviation of 1. The statistical significance of the correlation coefficient (r) is expressed by the two-tailed probability (p) where $p < 0.01$ results are considered to be of high statistical significance, $0.01 < p < 0.05$ of intermediate significance and $p > 0.05$ of low significance. Cluster analysis was performed with the Statistica 10 software to reveal similarities in sedimentological and geochemical compositions among the sediment samples. We used the Euclidean distance and the Ward method on the raw data set.

4. Results

4.1. Sedimentological properties

Fjord sediments are generally fine-grained and moderately to very poorly sorted (Fig. 2 and Supp. Fig. 1 and Supp. Table 1). The sand content in all analyzed samples varies between 1.8 and 79.8%, the silt fraction ranges from 18.6 to 85.4%, and the clay content rarely exceeds 10% (Table 4). Although the contents of sand and silt fractions vary the most, the majority of the samples, 86.4% on average, is mostly composed of medium silt to fine sand fractions (8-250 μm) (Supp. Table 1). Based on the Folk's (1954) scheme the samples are classified into three textural groups: silty sand ($n=96$), sandy silt ($n=165$) and silt ($n=11$) (Fig. 3). In general, coarser sediments characterize samples from the outer fjord (Fig. 3). Silty sand sediments dominate mostly at the SW part of the outer fjord and comprise all samples of cores 007, 010, 011 and 013 as well as the majority of samples from the bottom part of core 005 and the top part of core 1065. They are also found in cores from the NE part of the outer fjord and constitute 50% of samples in core 008, 17% in core 1075 and 13% in core 1087. Moreover, single samples are found in cores 002 and 1039. Sandy silt type sediments dominate in the NE outer fjord as well as in the inner fjord. In the NE outer fjord they constitute all samples of cores 003, 004, 009 as well as 87% of samples in core 1087, 83% in core 1075 and 50% in core 008. In the inner fjord, sandy silt sediments comprise all samples of core 1089, 95% of samples in core 002, 93% in core 1039, 70% in core 1079 and 60% in core 001. The least common silt type dominates in the inner fjord, specifically in the bottom part of core 001 (40% of samples) and at 6-13 cm depth in core 1079 (30% of samples). A single sample of silt type is also found at the bottom of core 1065 from the SW outer fjord. The frequency curves of sediment samples plotted as depth profiles for each core show nearly uniform trends with dominating unimodal grain size distribution (Fig. 4 and Supp. Fig. 2). In cores 001, 002, 1039, 1079 and 1089, retrieved from the inner fjord, an interval of bimodal distribution is found with one mode within the very coarse and one mode in the coarse silt fraction (31-63 μm and 16-31 μm , respectively). This interval is typically a few centimeters thick, mostly found at core depths between 3 and 14 cm, and it is more fine-grained compared to the over- and under-lying sediments. A similar pattern of increased mud content combined with non-unimodal distribution was also found in a few samples from the lowest part of cores 1065 and 1087 from the outer fjord. However, those sediments are of tri- to polymodal distribution.

4.2. Sediment geochemistry

The TOC contents vary between 0.03 to 1.9 wt% (Table 4). The highest average contents, i.e. >1 wt% occur in cores 001, 002, 003, 005, 009 and 011 (Fig. 2 and Supp. Fig. 1). In general, vertical changes of TOC content in most of the cores are relatively small. They typically increase slightly towards the core tops. The lowest TOC contents occur in an up to 10 cm thick interval terminating about 3 cm below the surface of the following cores from the inner fjord: 001, 002, 1039 and 1079.

The highest average concentrations (tens to hundreds of mg kg^{-1}) in all analyzed samples have Ni, V, Zn, Cr, Ba, Cu and Ti, whereas average concentrations of Pb, Co, As, Cd and Hg are lower (Table 4). The Hg concentration in 48% of the samples was below its detection limit (0.01 mg kg^{-1}) (Table 4, Fig. 2 and Supp. Fig. 1). Highest average concentrations of heavy metals occur in cores retrieved from the inner part of the fjord: As, Ba, Cd, Cu and Zn in core 1079; Pb, Ti and V in core 1089; Co, Cr, Ni in core 001; Hg in core 1039. Concentrations of Cu are the most variable for all measured heavy metals, in particular in cores from the inner fjord: 002, 1079, 1089, and in one core 003 from the outer fjord, where concentrations increase in an up to 10 cm thick interval 4-8 cm below the seafloor (Fig. 2 and Supp. Fig. 1). Pearson correlation calculated for all samples reveals strong positive correlations ($r > 0.7$) of high significance levels ($p < 0.01$) in two distinct groups of metals: Ba-Co-Cr-Cu-Ni and Pb-V-Zn (Table 5). Correlations calculated for samples of individual cores show the same pattern in cores 002, 1079 and 1089 from the inner fjord. A pattern of two similar distinct groups: Co-Cr-Cu-Ni and As-Pb-Ti-V-Zn ($r > 0.7$ and $p < 0.01$) is observed in cores 001 and 1039 (Supp. Table 2), also from the inner fjord. In the case of the cores from the outer fjord, correlations between measured metal concentrations are more diverse. However, in general they show positive correlations of $r > 0.6$ and $p < 0.01$ for a majority of metals, most often between Ba, Co, Cr, Cu, Hg, Ni, Pb, Ti, V and Zn. As and Cd show predominantly weak negative correlations of intermediate to low statistical relevance to the rest of the metals.

4.3. Geoaccumulation index

According to the classification based on the I_{geo} values after Müller (1969) (Table 3) the majority of highly contaminated sediments (classes >4) is found in the inner part of the fjord, whereas sediments from the outer fjord are mostly uncontaminated to moderately contaminated (classes <1) (Fig. 2 and Suppl. Fig. 1). Moreover, the concentrations of metals like Co, Pb, Ti, V and Zn reveal uncontaminated to moderate contamination (classes <1) in all of the investigated cores. Very few samples indicate moderate to strong contamination (classes 2 to 4) by Cd, Cu and Hg in cores 003, 1065 and 1087 from the outer fjord. In addition to a few moderately contaminated (class 2) samples by Cd, Cu and Hg in core 009 there is also one sample (9-10 cm depth) with moderate to very high contamination (classes 3-5) by all heavy metals excluding Hg. The highest contamination levels in sediments from the inner fjord are caused by Cu with strong to very high contamination (classes >4) detected at approximately 5-13 cm depth in cores 002, 1079 and 1089 as well as in the entire cores 001 and 1039. A similar distribution pattern but of lower contamination degree (classes 2-4) is also characteristic for Ba and Cr. Moreover, moderate to strong contamination (classes 2 and 3) by Hg was found in a majority of the sediment samples from this part of the fjord, whereas contamination of classes 3 and 4 by Cd is only seen in core 1079.

4.4. Sediment accumulation rates

All of the $^{210}\text{Pb}_{ex}$ activity profiles generally decrease with sediment depth but with near-uniform and/or decreased activities in surface sediments (≤ 5 -cm), representing a surface mixed layer (e.g. Jaeger et al., 1998) (Fig. 5). In addition, uniformly low activities occurred within approximately 7-cm-thick intervals ~6 cm below the tops of core 002 and 1079 from the inner fjord, representing depositional events (e.g. Jaeger et al., 1998). There is also a clear difference in measured activities at the core tops (≤ 5 -cm) between cores 001, 002, 003, 1079 and cores 005, 013, 1065, 1075. The $^{210}\text{Pb}_{ex}$ activities in the first set of cores are twice as high on average compared to the second set.

Table 6 summarizes the SARs that were calculated for intervals below the surface mixing layer. In cases where no significant changes in the shape of the $^{210}\text{Pb}_{ex}$ activity profiles were recognized, i.e. in cores 003, 005, 013, 1065 and 1075, the $^{210}\text{Pb}_{ex}$ values for the deepest interval were used resulting in the following SARs 1.1, 1.5, 0.7, 0.9 and 0.9 mm yr^{-1} , respectively. In cores from the inner fjord, i.e. 002 and 1079, with evidence of depositional events, SARs were calculated in three intervals to estimate their values before, during and after each event. They are as follows, core 002: 2.1, 2.5 and 1.9 mm yr^{-1} , core 1079: 3.6, 4.3 and 1.2 mm yr^{-1} , respectively. Core 001, also retrieved from the inner fjord, is only 10 cm long so that its $^{210}\text{Pb}_{ex}$ activity profile is incomplete, thus making the calculations of SARs using radionuclide methods less accurate. However, as an analogue to cores 002 and 1079 the lowermost sediments below 6 cm depth are interpreted as the uppermost parts of an event-deposition interval, allowing the estimation of the after-event-deposition SAR. This calculated SAR of 1.5 mm yr^{-1} is in good agreement with equivalent SARs estimated in cores 002 and 1079.

Similar to $^{210}\text{Pb}_{ex}$ the ^{137}Cs activities are generally higher in cores 001, 002, 003, 1079 compared to core 005, 013, 1065, 1075 (Fig. 5). Clear peaks in ^{137}Cs activities that could be related to the intensification of nuclear bomb testing at the beginning of 1960 or the Chernobyl disaster in 1986 are absent. Most profiles are blurred in shape, although some elevated activities in a peak-like form are visible in profiles of cores 001, 002, 003 and 1079. The observed peak-like features are assumed to be artefacts caused by increased SARs and surface mixing of the sediments, hence diluting ^{137}Cs activities. ^{137}Cs -derived SARs were calculated based on maximum penetration depth of ^{137}Cs excluding the depth of surface mixing layer recognized in $^{210}\text{Pb}_{ex}$ activity profiles. Although, some of the cores are characterized by deep penetration of low ^{137}Cs activities, possibly related to deep mixing/bioturbation, estimated SARs by both ^{210}Pb and ^{137}Cs methods are generally in good agreement (Table 6).

5. Discussion

5.1. The state of the sedimentological environment and heavy metal contamination levels

The inner and outer parts of Repparfjorden are characterized by two distinct sediment dispersal patterns. The inner fjord acts as a major depo-centre of sediments. Pre- and post-event deposition SARs in the inner basin are on average one order of magnitude higher than in the outer fjord (Table 6) and sediments are generally finer (Fig. 3). A doubling of $^{210}\text{Pb}_{ex}$ and ^{137}Cs activities (Fig. 5) in sediment cores from the inner to outer fjord indicates an additional large source of radionuclides from sediments entering from the river, causing a so-called focusing effect (Appleby, 1998). A similar pattern of increased radionuclide activities as well as dominance of finer sediments is also observed in core 003 from the outer fjord, in the vicinity of the sill. This indicates the strongest influence of riverine discharge among the investigated sediment cores of the outer fjord. Calculated SARs in the outer part of Repparfjorden (Table 6) are generally comparable to SARs reported for four marine sites in Finnmark County from Sørøya, Snefjord,

1 Porsangerfjorden (0.45-0.95 mm yr⁻¹) and Magerøya (0.64 up to 2.8 mm yr⁻¹) (Larsen et al., 2010). In light of these
2 results, the average SAR of 3.8 mm yr⁻¹ calculated for a sediment core from central Repparfjorden (Christensen et al.,
3 2011) (Fig. 1) may be overestimated.

4 The generally coarser granulometric composition in the outer fjord sediments (Fig. 2 and 3, Suppl. Fig. 1), combined
5 with lower SARs (Table 6), implies reduced sediment supply and/or a more intensive bottom current flow in this area
6 leading to non-deposition or winnowing of fine-grained material. The dominance of finer sediments – sandy silt type at
7 the northeastern part and coarser – silty sand at the southwestern part of the fjord would suggest relatively stronger
8 bottom currents at the southern side of the outer fjord. Christensen et al. (2011), conducted *in-situ* measurements of
9 bottom-current intensity for two short periods at nine stations along the southern and western shores of the fjord.
10 Stronger bottom currents were observed during the summer period with a predominately inflow direction. The observed
11 asymmetrical pattern in granulometric composition of the outer fjord sediments probably also reflect the influence of
12 the Coriolis Effect, leading to the counter-clockwise circulation (for details see e.g. Cottier et al., 2010).
13 Suspended/turbid sediments derived from Repparfjordelva are deflected to the right, looking towards the fjord mouth,
14 resulting in the observed transport/deposition of the sediments along the eastern and northern shores of the fjord. In
15 summary, it is suggested that the major portion of net outflow and major sediment transport at the bottom of the outer
16 fjord occurs along the northeastern side (compare with Plassen and Vorren, 2002).

17 Norwegian Pollution Control Authorities classify contaminants in marine sediments for ecotoxicological effects (SFT,
18 2007; Bakke et al., 2010). This classification system was developed on the basis of previous guidelines taking into
19 account the statistical distribution of contaminant levels found in soft sediments along coastal regions in Norway and is
20 in accordance with the risk assessment principles of the European Union (for details see Bakke et al., 2010). Five levels
21 of contamination are distinguished for the priority metals As, Cd, Co, Cr, Hg, Ni, Pb and Zn. Whereas class I is defined
22 as background contaminant level, classes II to V represent different levels of probable toxicity (Table 7). The border
23 between classes II and III is of critical importance for the assessment of sediment quality since it separates non-toxic
24 and toxic contamination levels (Bakke et al., 2010). This classification system was developed for fine-grained
25 sediments (mud fraction) and is regarded as not suitable for sediments containing gravel and coarse sand fractions. We
26 apply this classification in our study because the investigated sediment samples are dominantly composed of mud (clay
27 and silt) fraction (Table 4, Fig. 3) with an average content of 59.7%, whereas the majority of sand fraction is very fine
28 to fine (63-250 µm) (Supp. Table 1). The coarse and very coarse sand fractions (0.5-2 mm) rarely exceed 1% on
29 average and are only found in four cores (002, 004, 1065 and 1087). Moreover, we suggest that the assessment of
30 sediment quality should consider bulk sediments as that is how they are found in the natural environment.

31 In our study, the majority of the investigated sediments corresponds with class I representing background levels
32 following the I_{geo}-based classification indicating uncontaminated to moderately contaminated sediments (Fig. 2 and
33 Suppl. Fig. 1). Moreover, in almost all cases of moderate to strong contamination for As, Cd, Cr, Hg, and Ni those
34 levels are potentially not toxic for organisms according to the Norwegian sediment quality classification system (SFT,
35 2007). One of the exceptions is a sample from 9-10 cm depth of core 009 that represents class IV (bad state) for Cu and
36 Ni. However, Cu causes the highest and most frequent degree of contamination corresponding to classes IV and V,
37 representing levels potentially posing toxic effects after only short-term exposure. This is found in an approximately 13
38 cm-thick surface layer of all sediment cores from the inner fjord (Fig. 2 and Suppl. Fig. 1). In addition, in core 003 from
39 the outer fjord a 2 cm-thick sediment layer at ~7 cm core depth is of bad quality (class IV) due to Cu contamination. No
40 similar elevated levels of Cu were found in a core SED kjerne (Christensen et al., 2011) retrieved near core 003 (Fig. 1).

41 **5.1.1. Tailings dispersal record**

42 The geochemical and sedimentological records reveal some similar trends for the entire study area. A cluster analysis
43 was carried out to elucidate the lateral and vertical relationships among the studied variables. The set of samples used
44 for the cluster analysis includes all samples for which grain size, heavy metals and TOC concentrations were acquired.
45 Only concentrations of Ba, Co, Cr, Cu, Ni, Pb, V, Zn were chosen due to their specific correlation pattern (see section
46 4.2).

47 The cluster analysis revealed two main clusters *A* and *B*. In relation to the linkage distance the *B* cluster was also
48 subdivided into second-order sub-clusters: 1, 2 and 3 (Fig. 6). These cluster results along with the assessment of SARs
49 distinguish three types of sediments: those simultaneously deposited with mine tailings and affected most by the
50 disposal, hereafter called mine-tailing sediments; sediments affected by mine tailing disposal, called tailing-affected
51 sediments; and natural sediments, not affected by the disposal.

52 *Mine-tailing sediments.* The samples interpreted as mine-tailing sediments are equivalent to sub-clusters *B1* and *B2*
53 (*n*=8 and *n*=23, respectively). They are found only in cores from the inner fjord, the area of intended tailing disposal, at
54 the depths of 5-9 cm below the seafloor in cores 002, 1079 and 1089 as well as in bottom parts of cores 001 and 1039
55 (3-6 cm depth below the surface, respectively). The dominating anthropogenic origin of those sediments is deduced
56
57
58
59
60
61
62
63
64
65

1 from their geochemical signature, that is the highest concentrations of Ba, Co, Cr, Cu and Ni, among which Ba and Cu
2 indicate the highest degree of contamination, up to 760 and 1316 mg/kg (340 and 550 mg/kg on average), respectively
3 (Fig. 2, Suppl. Fig. 1). Following the Norwegian sediment quality classification (SFT, 2007) the observed Cu levels
4 correspond to the highest class of contamination indicating sediments of very bad state with concentration levels that
5 may pose severe acute toxic effects. The presence of elevated Ba content following the pattern of increased Cu
6 concentration is most likely related to the mineralogy of the mined ore formation. In the Repparfjord Tectonic Window
7 area barite (BaSO_4) was reported in vein structures (Viola et al., 2008; Vokes, 1956). Moreover, elevated Ba
8 concentrations, 551 mg/kg on average, characterize the newly processed tailings from the Ulveryggen formation (Kleiv,
9 2011). Alternative potential source of Ba is drill cuttings disposed in the old open pits of the Ulveryggen mine since
10 2005 (Ettner and Sanne, 2016). The Ba-based components are often used by petroleum industry at seafloor extraction
11 sites as a flocculent in drilling mud (for details see e.g. Lepland et al., 2000). However, there is no indication of elevated
12 Ba concentrations in the surface fjord sediments deposited during the last decade that could be linked to a potential
13 leakage of the drill cuttings. The occurrence of event-deposition layers with high SARs at almost the same depths in
14 cores 001, 002 and 1079, the layers deposited during the 1970s (Fig. 2, 5 and Table 6) further supports a tailing-origin.
15 Another geochemical feature of those sediments is the lowest TOC content (Fig. 2, Suppl. Fig. 1) indicating diluted flux
16 of the organic material due to higher SARs and/or suppressed biological activity during the time of deposition. The
17 tailing footprint is also clearly visible through the bimodal grain-size distribution (Fig. 2, 4 and Suppl. Fig. 2)
18 characteristic for the majority of the sediments grouped in cluster *B2*. This distribution suggests two ways of transport
19 and deposition. One of the modes, mostly the 1st mode (very coarse silt; 31-63 μm) is equivalent in size with a mode of
20 natural sediments recovered in the bottommost sections in a few cores from the inner fjord (see 'natural sediments'
21 paragraph and Fig. 4). Secondly, most often the 2nd mode (predominantly medium silt; 8-16 μm) is in the same fraction
22 size as sediments grouped in sub-cluster *B1* that are of unimodal distribution. Samples representing this sub-cluster are
23 only found in core 1079 which was taken in central part of the inner fjord from the site most proximal to the probable
24 tailings disposal outlet (Fig. 1). This pattern is accompanied by the highest concentrations of Cu (up to 1316 mg/kg),
25 which are comparable to the Cu concentrations for the newly produced Ulveryggen tailings (Kleiv, 2011). Therefore,
26 those sediments are interpreted to be mostly composed of mine tailings. Additionally, a specific spatial trend of the
27 bimodal distribution of the sediments from sub-cluster *B2* is observed. In cores 001 and 002 taken closer to core 1079
28 (most proximal to the past probable pipeline outlet location), the 1st mode is in the finer silt fraction ('tailings mode'),
29 whereas in more distant cores 1039 and 1089, the 1st mode is found in the coarser silt fraction ('natural mode'). This
30 trend is interpreted to reflect the spatially decreasing impact of the discharged tailings particles with increasing distance
31 from the probable outlet location in the inner fjord. In core 1089, the geochemical and sedimentological trends have a
32 vertical offset of approximately 2 cm. This is most likely related to the integration of two core duplicates for the
33 analyses performed (Table 1).

34 *Tailing-affected sediments.* The sediments interpreted as tailing-affected represent samples grouped in sub-cluster *B3*
35 ($n=37$). These are mostly found in cores from the inner fjord within a few centimeters-thick layer below the mine-tailing
36 sediments, as well as between the top of the mine-tailing sediments and seafloor. They are also found in the outer fjord
37 between 6-8 cm depth in core 003 located close to the sill, as well as in one sample from 9-10 cm depth in core 009 at
38 the northern side of the outer fjord. The geochemical and sedimentological signatures of those sediments indicate that
39 they were accumulated under an influence of disposed tailings. Tailing-affected sediments are characterized by elevated
40 concentrations of Ba, Co, Cr, Cu and Ni (Fig. 2 and Suppl. Fig. 1). The average Cu concentration of 120 mg/kg is
41 equivalent to IV class of sediments (bad state) according to the Norwegian quality classification (SFT, 2007) (Fig. 2 and
42 Suppl. Fig. 1). This level of contamination may pose toxic effects just after short-term exposure. Most of the tailing-
43 affected sediments are characterized by prevailing unimodal distribution of 'natural mode' with only a slightly
44 increased content of medium silt dominating in tailings sediments (Fig. 4 and Suppl. Fig. 2). Although one sample of
45 core 009 was grouped in sub-cluster *B3*, representing tailing-affected sediments, it is not regarded as such. This sample
46 is characterized by high concentrations of all of the measured heavy metals with an exception of Hg (Suppl. Fig. 1).
47 However, the TOC contents and the results of grain-size analysis do not indicate any excursions (Suppl. Fig. 1 and 2).
48 Therefore, this sample is assumed to be an outlier, perhaps accidentally contaminated prior to or during chemical
49 analyses.

50 *Natural sediments.* Sediments regarded as not affected by the tailings discharge, representing natural fjord sediments,
51 are grouped in cluster *A* ($n=193$). They constitute the majority of the investigated samples from cores taken in the outer
52 part of the fjord, as well as some sediment samples from lower parts of cores from the inner fjord (cores 002, 1079 and
53 1089). The geochemical signature of those sediments indicates that they are of natural background concentrations levels
54 (Fig. 2, Table 2) and, therefore, reflect local provenance. The observed variations in heavy metal concentrations are
55 mainly attributed to the varying grain-size composition (most likely related to the circulation pattern suggested
56 previously), a dependence that is also a natural feature of sediments (Loring, 1991). The down-core frequency profiles
57 show a dominating uniform unimodal pattern with the 1st mode in very coarse silt (31-63 μm) or very fine sand (63-125
58 μm) fractions (Fig. 4, Suppl. Fig. 2). Only the bottom sections of cores 1065 and 1087 contain sediments of tri- to
59 polymodal distributions (Fig. 4 and Suppl. Fig. 2). Those samples are composed mostly of finer sediments and are also
60 slightly enriched in almost all of the measured heavy metals (Fig. 2), reflecting the affinity of metals to the finer
61 fractions. It is assumed that the presence of those sediments represents a disturbance episode, most likely of
62
63
64
65

anthropogenic origin (e.g. anchoring, fishing) or a record of a gravity flow deposits in case of core 1087 located close to the shore, rather than sediments of different provenance.

5.2. The impact of mine tailings disposal

The impact of discharged mine tailings in Repparfjorden is mainly limited to a relatively small area of the inner fjord, the intended disposal site. The mine-tailing sediments restricted to the inner fjord are found along a ~1.5 km long transect. Sediments classified as tailing-affected are also found in a discrete 2-cm thick layer 6 cm below the top of core 003 from the outer fjord, indicating lateral spreading of tailings away from the discharge point. Core 003 is the most proximal to the sill among all cores from the outer fjord. Neither geochemical nor sedimentological records of the rest of the cores from the outer fjord, including the record of core SED kjerne (Christensen et al., 2011) (for location see Fig. 1), show potential influence of the tailings. Therefore, it is inferred that the spreading is spatially limited to the area about 1 km off the sill and about 2 km out from the probable discharge outlet. According to the recalculated SAR the spreading recorded in core 003 commenced before 1972 (Fig. 2). The $^{210}\text{Pb}_{\text{ex}}$ activity profile of this core shows 5-cm thick surface mixing layer (Fig. 5) limiting the usage of the radionuclide method for exact SAR calculations, hence also for dating purposes (see section 3.4). Since there are no other documented sources of Cu in the Repparfjorden area (with metal loads similar to level of the tailings) that could potentially have been active before the 1970s, it is deduced that the spreading actually took place during the time of disposal.

The tailings had the biggest influence on the investigated sediments of the inner fjord during the time of discharge, causing increased SARs and changes in sediment properties (e.g. bimodality). Furthermore, the geochemical record indicates the highest reported heavy metal concentrations in the same layers, mainly represented by Cu. However, even if the impacts of the tailings are restricted in the lateral dimension, the effects of tailings disposal are still significant, especially in the vertical dimension, i.e. in tailing-affected sediments found below and above mine-tailing sediments. The impact of tailings, visible in the geochemical record, is even found in the surface sediment layers, where Cu concentrations remain at an elevated level, representing bad sediment quality according to the Norwegian quality classification (SFT, 2007). On the other hand, the sedimentological properties of those sediments are more similar to the natural pre-disposal sediments. The observed pattern of the tailings impact decreasing gradually towards the top sections of inner fjord sediment cores indicates physical and/or biological reworking of the sediments after and/or during deposition. After disposal, resuspended mine-tailing sediments (due to natural processes) may release heavy metals to the water column either in the form of suspended particulate matter or in dissolved form (Durán et al., 2012; Xu et al., 2015). With the continuous transport and deposition of natural sediments from Repparfjordelva the released metals may afterwards be mixed (and re-precipitated) to sediments and finally deposited. The combination of a stronger geochemical and weaker sedimentological signal may also indicate remobilization (desorption) and dispersion of Cu within the water phase. Some of the metals, like Cu, have been reported to diffuse out and be transported within the sediment column through pore water under specific conditions (Blasco et al., 2000; Cheevaporn et al., 1995). Moreover, the study of Pedersen et al. (2016) on Cu availability in a 10-cm-thick sediment sample from the inner fjord indicate that about 80% of this metal is bound to more available fractions that are exchangeable, oxidisable and reducible. Consequently, the diagenetic processes like metal diffusion cannot be excluded. However, more detailed chemical studies are needed to elucidate the observed pattern.

From a toxicity perspective the ecological communities of the inner fjord have been continuously exposed to Cu concentrations that may pose toxic effects after short-term exposure for nearly 40 years. This level of exposure is potentially of high significance for benthic communities, especially for infaunal organisms. Previous studies on macrofaunal benthic communities in Repparfjorden are limited to surface samples only (Christensen et al., 2011; Dahl-Hansen and Velvin, 2008). In these earlier studies, benthic diversity did not indicate significant differences between the inner and outer fjord, despite, Cu concentrations in surface sediments representing bad sediment quality. There is a need for further studies in a broader scope that would include micro- and infaunal benthic communities, as well as detailed chemical investigations on the binding pattern of metals, their bioavailability and their changes with time and depth.

5.3. Potential long-term effects of tailings disposal

Lateral and vertical spreading of discharged tailings is mainly controlled by two factors: morphology of the fjord bottom and sediment accumulation. The morphological factor has played a crucial role in limiting the lateral redistribution of tailings. Due to the presence of the sill, the inner fjord environment constitutes a semi-enclosed basin, hence also a sink for the mine tailings deposited over time. Although, the bottom current strength in the outer fjord seems to be relatively high, potentially facilitating the spreading of tailings, the sill acts as a natural barrier. We identified only one discrete layer influenced by tailings in the outer fjord. On the contrary, the second factor – sediment accumulation has played a principal role in shaping the vertical distribution of tailings in Repparfjorden. The inner fjord basin constitutes a major depo-centre for (natural) sediments transported by the Repparfjordelva to the head of the fjord, resulting in SARs up to 2-3 times higher than in the outer fjord. This relatively high SAR downgraded the potential

1 impact of the disposal operations simply by diluting the tailing-related pollutants in the natural sediments. The average
2 post-disposal SAR in the inner fjord is of 1.5 mm yr^{-1} , meaning that after the cessation of the disposal, during the last 37
3 years (time between the cessation and average timing of core retrieval), the layer of 5.6 cm-thick sediments on average
4 was deposited. During this time, the Cu concentrations in the core taken close to the probable pipeline outlet (core
5 1079) decrease from 606 mg/kg (the topmost sample of mine-tailing sediments) to 84 mg/kg (the surface tailing-
6 affected sediments). Taking into consideration the average concentration for the entire inner fjord, the Cu
7 concentrations decrease accordingly from 308 to 98 mg/kg.

8 As postulated by Skei (2013), the prospective submarine disposal sites “should ideally be deep ($>100 \text{ m}$), flat or slightly
9 sloping bottom and surrounded by sills to make an enclosed basin where sedimentation is prominent”. Those features
10 are mostly met in Repparfjorden. The present study, conducted nearly 40 years after the cessation of tailings disposal,
11 proves that the distribution of tailings is spatially restricted to the intended disposal area. However, the natural
12 characteristics of fjords do not always ensure limited spreading of the discharged mine tailings. Among the most well-
13 studied fjord disposal sites are two sites from British Columbia (Canada): the Portland Canal-Observatory Inlet system
14 where molybdenum-lead-zinc tailings from Kitsault Mine were disposed (e.g. Odhiambo et al., 1996) and Rupert,
15 Holberg and Quatsino Sund system with discharged copper tailings from Island Copper Mine (e.g. Poling et al., 2002);
16 as well as the Uummannaq Fjord complex, West Greenland, where lead-zinc tailings from the Black Angel Mine were
17 disposed (e.g. Perner et al., 2010). A direct comparison of these fjord tailings disposal sites with the present work is not
18 possible, due to different fjords and tailings characteristics, as well as the application of different methods. Nonetheless,
19 in the West Greenland fjord, the tailing-related contaminants were detected 12 km from the mine, with environmental
20 consequences found beyond the intended disposal areas (e.g. Søndergaard et al., 2011).

21 Looking at a present-to-future scenario, any significant change in the controlling factors has a potential to re-shape the
22 observed impact of tailings in Repparfjorden. Although it is not feasible to speculate about the timing and magnitude of
23 such changes, processes that may influence the fjord bathymetry and water-mass properties, as well as changes in the
24 amount of sediments transported by Repparfjordelva are potentially important in a long-term perspective.

25 The prospective future spreading of the tailing-contaminated sediments would need to involve a strong enough bottom
26 current to trigger resuspension. Entrainment of contaminated sediments into the water column would need to occur
27 along with a change in the inner-outer fjord water exchange pattern to enable the transport of tailings over the sill and
28 into the outer fjord. The lack of elevated Cu concentrations and finer-grained sediments typical for mine-tailings
29 sediments in the surface layers of the outer fjord indicate that such processes have not taken place since the cessation of
30 tailings disposal. However, to rule out this possibility, there is a need for i) a monitoring survey focused on the present-
31 day Repparfjorden hydrography, as well as ii) a study of the paleo-record (millennial-timescale), to predict possible
32 patterns and rates of exchange between the inner and outer fjord.

33 The last of the mentioned changes that might influence the future effects of the disposed tailings is a change in the
34 amount of sediments accumulated in the inner part of the fjord. The average post-disposal SAR resulted in an
35 accumulation of about 5.6 cm-thick sediment layer, within which the average Cu concentrations dropped by $\sim 70\%$ to 98
36 mg/kg. If the SAR was 0.5 mm yr^{-1} lower, similar to the average outer fjord rate, based on linear interpolation between
37 the recorded average Cu concentrations found at different types of sediments in the inner fjord, then the Cu level of 98
38 mg/kg would be reached in 2034 resulting in an additional ~ 2 -cm thick layer of sediments. On the contrary, if the SAR
39 was higher, similar to the pre-disposal rate, then those Cu levels would have been reached earlier. Although this
40 calculation is a simplification of the natural fjord conditions, even a seemingly small change in SAR of 0.5 mm yr^{-1} has
41 a large potential to influence the environmental impacts of the disposed tailings on a human-timescale.

42 6. Conclusions

43 We assessed the state of the sedimentary environment and the effects of submarine Cu mine tailings disposal in the
44 1970s in Repparfjorden, northern Norway, based on sedimentological and geochemical analyses of seventeen short
45 sediment cores. We found that:

- 46 – The inner and outer parts of the fjord represent two distinct environmental settings. The inner fjord confined by
47 a sill is a depo-centre for contaminated mine tailings. The grain-size distribution pattern of sediments in the
48 outer fjord suggest counter-clockwise circulation of bottom currents.
- 49 – The mine-tailing sediments were found only in cores of the inner fjord along a $\sim 1.5 \text{ km}$ long transect. They
50 constitute an up to 9-cm thick layer, 3-9 cm below the core tops. It is composed of mostly silty sediments of
51 bimodal distribution characterized by the highest observed Cu concentrations (up to 1316 mg/kg and 550
52 mg/kg on average) and low TOC contents. The strongest influence of the mine tailings occurred in the central
53 part of the inner fjord, close to the location of the probable tailing outlet.

- 1
2
3
4
5
6
7
8
9
10
11
12
13
14
15
16
17
18
19
20
21
22
23
24
- The distribution pattern of tailing-affected sediments implies that dispersion of tailing-related metals and particles is restricted to a relatively small area of the inner fjord to the immediate surrounding sediments and to a discrete layer in one core from the outer fjord most proximal to the sill. These sediments exhibit elevated Cu concentrations (120 mg/kg on average). Cu concentrations in sediment cores from the inner fjord gradually decrease towards the top core sections, implying physical and/or biological reworking of the sediments after and/or during deposition. Moreover, the lack of a clear tailings signal in the sedimentological record indicates that dispersion of Cu in the water phase is likely.
 - The presence of tailing-affected sediments in layers up to the sediment-water interface indicate that the ecological communities of the inner fjord have been exposed to concentrations of Cu for nearly 40 years.
 - The dispersal of tailings is mainly controlled by two factors: fjord morphology and sedimentation rate. Although, the strength of the bottom currents in the outer fjord seems to be relatively high, potentially facilitating the spreading of the tailings, the sill is acting as an effective natural barrier for the discharged tailings. The relatively high post-disposal SAR in the inner fjord downgraded the potential impact of the tailings disposal by diluting the tailing-related pollutants in the natural sediments.
 - The pattern of bimodal grain-size distribution along with increased content of finer tailing-related fraction in sediments of unimodal distribution facilitated the assessment of tailings discharge impact and allowed to track the spreading of the tailing particles.
 - There is a need for further studies to simultaneously address micro- and infaunal benthic communities and Cu bioavailability in order to provide an insight into the environmental/toxic effects of elevated Cu concentrations observed in sediment cores from the inner fjord. Moreover, a detailed investigation of the present and past hydrography in Repparfjorden is needed to answer the question of the inner-outer fjord water exchange pattern that may in the future contribute to the spreading of tailing-affected sediments.

25 Acknowledgements

26
27
28
29
30
31
32
33
34
35

The authors would like to thank the captains and crews of R/V Helmer Hanssen as well as cruise engineers: B.R. Olsen, S. Iversen, and all of the scientific participants of the two cruises for a help in coring and core sampling. T.M. Dahl, I. Hald and K. Monsen kindly assisted with laboratory works. T. Grytå helped with Fig. 1. This study was conducted mainly within the Environmental Waste Management (EWMA) project funded by the Research Council of Norway through NORDSATSING (grant number: 195160), EniNorge AS and the UiT The Arctic University of Norway in Tromsø.

36 References

- 37
38
39
40
41
42
43
44
45
46
47
48
49
50
51
52
53
54
55
56
57
58
59
60
61
62
63
64
65
- Appleby, P.G., 1998. Dating Recent Sediments by ^{210}Pb : Problems and Solutions. In: Proceedings of STUK Symposium, Helsinki, STUK-A145, 7–24.
- Bakke, T., Källqvist, T., Ruus, A., Breedveld, G.D., Hylland, K. 2010. Development of sediment quality criteria in Norway. *J. Soil Sediment.* 10, 172–178.
- Barbanti, A., Bothner, M.H., 1993. A procedure for partitioning bulk sediments into distinct grain-size fractions for geochemical analysis. *Environ. Geol.* 21, 3–13.
- Blasco, J., Sáenz, V., Gómez-Parra A., 2000. Heavy metal fluxes at the sediment-water interface of three coastal ecosystems from south-west of the Iberian Peninsula. *Sci. Total Environ.* 247, 189–199.
- Boltt, S.J., Pye, K., 2001. Gradistat: a grain size distribution and statistics package for the analysis of unconsolidated sediments. *Earth. Surf. Proc. Land.* 26, 1237–1248.
- Brook, E.J., Moore, J.N., 1988. Particle-size and chemical control of As, Cd, Cu, Fe, Mn, Ni, Pb, and Zn in bed sediment from the Clark Fork River, Montana (U.S.A.). *Sci. Total Environ.* 76, 247–266.
- Burd, B.J., 2002. Evaluation of mine tailings effects on a benthic marine infaunal community over 29 years. *Mar. Environ. Res.* 53, 481–519.
- Carroll, J., Lerche, I., 2003. *Sedimentary Processes: Quantification using Radionuclides*. Elsevier, 250 pp.
- Cheevaporn, V., Jacinto, G.S., San Diego-McGlone M.L., 1995. Heavy Metal Fluxes in Bang Pakong River Estuary, Thailand: Sedimentary vs Diffusive Fluxes. *Mar. Pollut. Bull.* 31, 4–12.

Christensen, G.N., Dahl-Hansen, G.A.P., Gaarsted, F., Leikvin, Ø., Palerud, R., Velvin, R., Vögele, B., 2011. Marin grunnlagsundersøkelse i Repparfjorden, Finnmark 2010–2011. Akvaplan-niva report No. 4973-1, Tromsø, Norway, 118 pp.

Cottier, F. R., Nilsen, F., Skogseth, R., Tverberg, V., Skardhamar, J., Svendsen, H., 2010. Arctic fjords: a review of the oceanographic environment and dominant physical processes. In: Howe, J.A., Austin, W.E.N., Forwick, M., Paetzel, M. (eds). *Fjord Systems and Archives*. Geological Society, London, Special Publications: 344: 289–304.

Dahl-Hansen, G.A.P., Velvin, R., 2008. Resipientundersøkelse/grunnlagsundersøkelse i Repparfjorden. Akvaplan-niva rapport No. 4157 – 01, Tromsø, Norway, 53 pp.

Dijkstra, N., Junttila, J., Skirbekk, K., Carroll, J., Husum, K., Hald, M., 2016. Benthic foraminifera as bio-indicators of chemical and physical stressors in Hammerfest harbor (Northern Norway). *Mar. Pollut. Bull.* <http://dx.doi.org/10.1016/j.marpolbul.2016.09.053>.

Durán, I., Sánchez-Martín, P., Beiras, R., 2012. Dependence of Cu, Pb and Zn remobilization on physicochemical properties of marine sediments. *Mar. Environ. Res.* 77, 43–49.

Edinger, E.N., Siregar, P.R., Blackwood, G.M., 2007. Heavy metal concentrations in shallow marine sediments affected by submarine tailings disposal and artisanal gold mining, Buyat-Ratototok district, North Sulawesi, Indonesia. *Environ. Geol.*

Edinger, E., 2012. Gold mining and submarine tailings disposal: Review and case study. *Oceanography* 25, 184–199.

Elberling, B., Knudsen, K.L., Kristensen, P.H., Asmund, G., 2003. Applying foraminiferal stratigraphy as a biomarker for heavy metal contamination and mining impact in a fjord in West Greenland. *Mar. Environ. Res.* 55, 235–256.

Ettner, D.C., Sanne, E.H., 2016. Potential for mine water contamination after cessation of mining at Nussir. Geode Consult AS report, Asker, 13 pp.

Folk, R.L., 1954. The Distinction between Grain Size and Mineral Composition in Sedimentary-Rock Nomenclature. *J. Geol.* 62, 344–359.

Hughes, D.J., Shimmield, T.M., Black, K.D., Howe, J.A., 2015. Ecological impacts of large-scale disposal of mining waste in the deep sea. *Scientific Reports* 5, 09985. Doi: 10.1038/srep09985.

IMO, 2016. London Convention and Protocol: Convention on the Prevention of Marine Pollution by Dumping of Wastes and Other Matter, London, UK. <http://www.imo.org/en/OurWork/Environment/LCLP/Pages/default.aspx>. Accessed 7 September 2016.

Islam, M.S., Tanaka, M., 2004. Impacts of pollution on coastal and marine ecosystems including coastal and marine fisheries and approach for management: a review and synthesis. *Mar. Pollut. Bull.* 48, 624–649.

Jaeger, J.M., Nittroer, C.A., Scott, N.D., Milliman, J.D., 1998. Sediment accumulation along a glacially impacted mountainous coastline: north-east Gulf of Alaska. *Basin Res.* 10, 155–173.

Josefson, A.B., Hansen, J.L.S., Asmund, G., Johansen, P., 2008. Threshold response of benthic macrofauna integrity to metal contamination in West Greenland. *Mar. Pollut. Bull.* 56, 1265–1274.

Kleiv, R.A., 2011. Fysiske og kjemiske egenskaper til flotasjonsavgang fra Nussir- og Ulveryggen-forekomstene. En supplert sammenstilling av laboratorieresultater fra SGS Mineral Services, Canada. NTNU report No. M-RAK 2011,7, Trondheim, 25 pp.

Kvassnes, A.J.S., Iversen, E., 2013. Waste sites from mines in Norwegian fjords. *Mineralproduksjon* 3, A27–A38.

Larsen, T.S., Kristensen, J.A., Asmund, G., Bjerregaard, P., 2001. Lead and zinc in sediments and biota from Maarmorilik, West Greenland: an assessment of the environmental impact of mining wastes on an Arctic fjord system. *Environ. Pollut.* 114, 275–283.

Larsen, J., Appleby, P.G., Christensen, G.N., Berg, T., Eide, I., 2010. Historical and Geographical Trends in Sediment chronology from Lakes and Marine Sites Along the Norwegian Coast. *Water Air Soil Pollut.* 206, 237–250.

Lepland, A., Sæther, O.M., Thorsens, T., 2000. Accumulation of barium in recent Skagerrak sediments: sources and distribution control. *Mar. Geol.* 163, 13–26.

Little, M.E., Parsons, M.B., Law, B.A., Milligan, T.G., Smith, J.N., 2015. Impact of historical gold mining activities on marine sediments in wine Harbour, Nova Scotia, Canada. *Atlantic Geol.* 51, 344–363.

Loring, D.H., 1991. Normalization of heavy-metal data from estuarine and coastal sediments. *ICES J. Mar. Sci.* 48, 101–115.

1 Loring, D.H., Rantala, R.T.T., 1992. Manual for the geochemical analyses of marine sediments and suspended
2 particulate matter. *Earth-Sci. Rev.* 32, 235–283.

3
4 Marthinussen, M., 1960. Brerandstadier og avsmeltningsforhold i Repparfjorden- Stabbursdal-området, Finnmark.
5 Norges Geologiske Undersøkelse Årbok 216, 118–169.

6
7 Martínez, M.L., Intralawan, A., Vázquez, G., Pérez-Maqueo, O., Sutton, P., Landgrave, R., 2007. The coasts of our
8 world: Ecological, economic and social importance. *Ecol. Econ.* 63, 254–272.

9 Müller, G., 1969. Index of geoaccumulation in the sediments of the Rhine River. *Geojournal* 2, 108–118.

10
11 Norwegian Standard, 1989. NS 4768: Water analysis - Determining of mercury by cold vapour atomic absorption
12 spectrometry.

13
14 Norwegian Standard, 1994. NS 4770: Water analysis - Determination of metals by atomic absorption
15 spectrophotometry, atomization in flame - General principles and guidelines.

16
17 Odhiambo, B.K., Macdonald, R.W., O'Brien, M.C., Harper, J.R., Yunker, M.B., 1996. Transport and fate of mine
18 tailings in a coastal fjord of British Columbia as inferred from the sediment record. *Sci. Total Environ.* 191, 77–94.

19
20 Okada, T., Larcombe, P., Mason, C., 2009. Estimating the spatial distribution of dredged material disposed of at sea
21 using particle-size distributions and metal concentrations. *Mar. Pollut. Bull.* 58, 1164–1177.

22
23 Ottesen, R.T., Bogen, J., Bølviken, B., Volden, T., 1989. Overbank sediment: a representative sampling medium for
24 regional geochemical mapping. *J. Geochem. Explor.* 32, 257–277.

25
26 Ottesen, R.T., Bogen, J., Bølviken, B., Volden, T., Haugland, T., 2000. Geokjemisk atlas for Norge, del 1: Kjemisk
27 sammensetning av flomsedimenter. NGU, Trondheim, 140 pp.

28
29 Pedersen, K.B., Jensen, P.E., Ottosen, L.M., Evenset, A., Christensen, G.N., Frantzen, M., 2016. Metal speciation of
30 historic and new copper mine tailings from Repparfjorden, Northern Norway, before and after acid, base and
31 electrolytic extraction. *Miner. Eng.*, <http://dx.doi.org/10.1016/j.mineng.2016.10.009>.

32
33 Perner, K., Leipe, T., Dellwig, O., Kuijpers, A., Mikkelsen, N., Andersen, T.J., Harff, J., 2010. Contamination of arctic
34 Fjord sediments by Pb–Zn mining at Maarmorilik in central West Greenland. *Mar. Pollut. Bull.* 60, 1065–1073.

35
36 Plassen, L., Vorren, T.O., 2002. Late Weichselian and Holocene sediment flux and sedimentation rates in Andfjord and
37 Vågsfjord, North Norway. *J. Quaternary Sci.* 17, 161–180.

38
39 Poling, G.W., Ellis, D.V., Murray, J.W., Parson, T.R., Pelletier C.A., 2002. Underwater Tailing Placement at Island
40 Copper Mine: A Success Story. Society for Mining, Metallurgy and Exploration, Inc. (SME), USA, 204 pp.

41
42 Ramirez-Llodra, E., Trannum, H.C., Evenset, A., Levin, L.A., Andersson, M., Finne, T.E., Hilario, A., Flem, B.,
43 Christensen, G., Schaanning, M., Vanreusel, A., 2015. Submarine and deep-sea mine tailing placements: A review of
44 current practices, environmental issues, natural analogs and knowledge gaps in Norway and internationally. *Mar. Pollut.*
45 *Bull.* 97, 13–35.

46
47 Ridgway, J., Shimmield, G., 2002. Estuaries as Repositories of Historical Contamination and their Impact on Shelf
48 Seas. *Estuar. Coast. Shelf S.* 55, 903–928.

49
50 Robbins, J.A., Edgington, D.N., 1975. Determination of recent sedimentation rates in Lake Michigan using Pb-210 and
51 Cs-137. *Geochim. Cosmochim. Ac.* 39, 285–304.

52
53 Sandstad, J.S., Bjerkgård, T., Boyd, R., Ihlen, P., Korneliussen, A., Nilsson, L.P., Often, M., Eilu, P., Hallberg, A.,
54 2012. Metallogenic areas in Norway. In: Eilu, P. (Eds.), *Mineral deposits and metallogeny of Fennoscandia*. *Geol. S,*
55 *Finl.* 53, 35–138.

56
57 SFT, 2007. Veileder for klassifisering av miljøkvalitet i fjorder og kystfarvann. Revidering av klassifisering av metaller
58 og organiske miljøgifter i vann og sedimenter (Guidelines for classification of environmental quality in fjords and
59 coastal areas. Revision of classification of metals and organic contaminants in water and sediment). Norwegian
60 Pollution Control Authority SFT TA-2229/2007.

61
62 Skei, J.M., 2013. The dilemma of waste management in the mining industry – criteria for sea disposal.
63 *Mineralproduksjon* 3, B1–B4.

64
65

Søndergaard, J., Asmund, G., Johansen, P., Rigét, F., 2011. Long-term response of an arctic fiord system to lead-zinc mining and submarine disposal of mine waste (Maarmorilik, West Greenland). *Mar. Environ. Res.* 71, 331–341.

1 Syvitsky, J.P.M., Burrell, D.C., Skei, J.M., 1987. *Fjords. Processes and products*. Springer, New York, 379 pp.

2
3 Szczuciński, W., Jagodziński, R., Hanebuth, T.J.J., Stattegger, K., Wetzel, A., Mitreğa, M., Unverricht, D., Van Phach,
4 P., 2013. Modern sedimentation and sediment dispersal pattern on the continental shelf off the Mekong River delta,
5 South China Sea. *Global Planet. Change.* 110, 195–213.

6
7 Viola, G., Snadstad, J.S., Nilsson, L.P., Heincke, B., 2008. Structural and ore geological studies in the northwestern part
8 of the Repparfjord Window, Kvalsund, Finnmark, Norway. *Norges Geologiske Undersøkelse rapport No. 2008.029*,
9 Trondheim, Norway, 93 pp.

10 Vogt, C., 2013. *International Assessment of Marine and Riverine Disposal of Mine Tailings. Final Report Adopted by*
11 *the International Maritime Organization, London Convention/Protocol, IMO.*

12
13 Vokes, F.M., 1956. Some copper sulphide parageneses from the Raipas formation of Northern Norway. *Norges*
14 *Geologiske Undersøkelse Årbok* 200, 74–111.

15
16 Vøllestad, L.A., Skurdal, J., L'abée-Lund, J.H., 2014. Evaluation of new management scheme for Norwegian Atlantic
17 salmon *Salmo salar*. *Fisheries Manag. Ecol.* 21, 133–139.

18
19 Xu, W., Li, X., Wai, O.W.H., Huang, W., Yan, W., 2015. Remobilization of trace metals from contaminated marine
20 sediment in a simulated dynamic environment. *Environ. Sci. Pollut. Res.* 22, 19905–19911.

21
22 Zonta, R., Zaggia, L., Argese, E., 1994. Heavy metal and grain-size distributions in estuarine shallow water sediments
23 of the Cona Marsh (Venice Lagoon, Italy). *Sci. Total Environ.* 151, 19–28.

24
25
26
27
28
29
30
31
32
33
34
35
36
37
38
39
40
41
42
43
44
45
46
47
48
49
50
51
52
53
54
55
56
57
58
59
60
61
62
63
64
65

Table(s)

Table 1. Overview of the coring stations (core-ID, coring gear, sampling date, location, water depth, recovery, number of 1-cm thick samples per core) and overview of analyses performed (grain size; HM; heavy metals concentration; TOC; total organic carbon content; radioisotopes: ²¹⁰Pb and ¹³⁷Cs activities). Analyses of HM and TOC marked with * were conducted at the Technical University of Denmark. The remaining TOC measurements were performed at the Department of Geosciences, UiT The Arctic University of Norway in Tromsø, whereas the remaining HM analyses were carried out at Unilab Analyse AS (Tromsø, Norway). SED kjerne from Christensen et al. (2011).

Station No	Core-ID	Coring gear	Sampling date	Latitude (N)	Longitude (E)	Approximate core location within the fjord	Water depth (m)	Recovery (cm)	Number of samples	Analyzed parameters
HH13-001-MC-MF-D	001	multi corer	16.04.2013	70°27.611'	024°17.516'	inner	47	10	10	Grain size, HM, TOC*, radioisotopes
HH13-002-MC-MF-D	002	multi corer	16.04.2013	70°28.383'	024°17.737'	inner	63	21	21	Grain size, HM, TOC*, radioisotopes
HH13-003-MC-MF-D	003	multi corer	16.04.2013	70°29.211'	024°16.537'	outer	86	20	20	Grain size, HM, TOC*, radioisotopes
HH13-004-MC-MF-D	004	multi corer	16.04.2013	70°29.867'	024°14.996'	outer	59	15	15	Grain size, HM, TOC
HH13-005-MC-MF-D		multi corer	16.04.2013	70°29.388'	024°14.041'	outer	53	20	20	HM, TOC*
HH13-005-MC-MF-E	005	multi corer	16.04.2013	70°29.388'	024°14.041'	outer	53	19	19	Grain size
HH13-007-MC-MF-E	007	multi corer	16.04.2013	70°30.042'	024°12.180'	outer	60	10	10	Grain size, HM, TOC
HH13-008-MC-MF-D	008	multi corer	16.04.2013	70°30.427'	024°12.916'	outer	65	8	8	Grain size, HM, TOC
HH13-009-MC-MF-D	009	multi corer	16.04.2013	70°31.028'	024°10.108'	outer	83	20	20	HM, TOC*
HH13-009-MC-MF-E		multi corer	16.04.2013	70°31.028'	024°10.108'	outer	83	20	20	Grain size
HH13-010-MC-MF-D	010	multi corer	16.04.2013	70°30.552'	024°09.357'	outer	74	11	11	Grain size, HM, TOC
HH13-011-MC-MF-D	011	multi corer	16.04.2013	70°29.954'	024°08.883'	outer	114	18	18	Grain size
HH13-011-MC-MF-E		multi corer	16.04.2013	70°29.954'	024°08.883'	outer	114	20	20	HM, TOC*
HH13-013-MC-MF	013	multi corer	16.04.2013	70°30.886'	024°06.695'	outer	115	13	13	Grain size, HM, TOC, radioisotopes
IG15-1-1039-BCA	1039	box corer	23.06.2015	70°27.566'	024°17.178'	inner	44	14.5	15	Grain size
IG15-1-1039-BCB		box corer	23.06.2015	70°27.566'	024°17.178'	inner	44	12	12	HM, TOC
IG15-1-1065-BCA	1065	box corer	24.06.2015	70°30.075'	024°11.350'	outer	51	19	19	Grain size, HM*
IG15-1-1065-BCB		box corer	24.06.2015	70°30.075'	024°11.350'	outer	51	15	15	TOC*, radioisotopes
IG15-1-1075-MCA	1075	multi corer	24.06.2015	70°29.462'	024°15.079'	outer	72	18.5	18	Grain size
IG15-1-1075-MCB		multi corer	24.06.2015	70°29.462'	024°15.079'	outer	72	16.5	16	HM, TOC, radioisotopes
IG15-1-1079-MCA	1079	multi corer	24.06.2015	70°28.153'	024°17.530'	inner	61	20	20	Grain size
IG15-1-1079-MCB		multi corer	24.06.2015	70°28.153'	024°17.530'	inner	61	20	20	HM*, TOC*, radioisotopes
IG15-1-1087-BCA	1087	box corer	24.06.2015	70°30.561'	024°12.885'	outer	65	14.5	15	Grain size
IG15-1-1087-BCB		box corer	24.06.2015	70°30.561'	024°12.885'	outer	65	14	14	HM*, TOC*
IG15-1-1089-MCA	1089	multi corer	24.06.2015	70°28.397'	024°17.999'	inner	57	20	20	Grain size
IG15-1-1089-MCB		multi corer	24.06.2015	70°28.397'	024°17.999'	inner	57	20	20	HM, TOC
SEDkjerne			2010	70°29.380'	024°15.681'	outer	88	17	7	Grain size, HM, TOC, radioisotopes

Table 2. Heavy metals background values. Levels 1, 2 and 3 are from this study (Hg* background levels equal to its detection limit); SED kjerne from Christensen et al. (2011); overbank sediments from Ottesen et al. (2000).

Background	Mud [%]	As [mg/kg]	Cd [mg/kg]	Co [mg/kg]	Cr [mg/kg]	Cu [mg/kg]	Hg* [mg/kg]	Ni [mg/kg]	Pb [mg/kg]	V [mg/kg]	Zn [mg/kg]	Ba [mg/kg]	Ti [mg/kg]
Level 1	66	3.0	0.06	4.2	23	10.0	0.01	13.3	4.4	18	21	32	700
Level 2	52	2.2	0.04	3.4	20	11.2	0.01	10.1	3.6	15	16	29	658
Level 3	40	2.3	0.06	3.1	17	6.2	0.01	9.7	2.7	14	14	24	525
SED kjerne	73	-	<0.2	-	11	-	-	-	3.6	-	20	-	-
Overbank sediments	100	≤6	-	≤25	≤100	≤16	-	≤16	≤16	≤32	≤39	-	-

Table 3. Descriptive classes of the contaminations degree based on the geoaccumulation index (I_{geo}) values (Müller 1969).

I_{geo} value	I_{geo} class	Description
<0	0	uncontaminated
0-1	1	uncontaminated to moderately contaminated
1-2	2	moderately contaminated
2-3	3	moderately to strongly contaminated
3-4	4	strongly contaminated
4-5	5	strongly to extremely contaminated
>5	6	extremely contaminated

Table 4. Statistics for grain-size, total organic carbon content (TOC) and heavy metals (As, Ba, Cd, Co, Cr, Cu, Hg, Ni, Pb, Ti, V and Zn) concentrations for all investigated sediment cores (for locations see Figure 1).

Core-ID	Sand [vol. %]	Silt [vol. %]	Clay [vol. %]	TOC [wt. %]	As [mg/kg]	Cd [mg/kg]	Co [mg/kg]	Cr [mg/kg]	Cu [mg/kg]	Hg [mg/kg]	Ni [mg/kg]	Pb [mg/kg]	V [mg/kg]	Zn [mg/kg]	Ba [mg/kg]	Ti [mg/kg]
001	Min	4.8	70.5	6.3	0.26	0.01	7.7	68	126.0	0.034	23.9	2.5	16	18	118	574
	Max	23.3	83.9	11.3	1.66	0.06	9.8	147	310.0	0.047	37.6	9.8	39	36	198	1440
	Mean	12.1	78.8	9.0	1.02	0.04	8.5	111	237.3	0.038	31.4	6.5	27	28	155	978
	Median	10.9	79.9	9.2	1.12	0.04	8.4	109	237.5	0.037	32.0	7.6	31	33	152	1110
002	Min	11.4	45.2	3.3	0.55	0.02	3.0	17	13.8	<0.01	9.1	3.4	11	15	24	417
	Max	51.6	78.6	10.0	1.74	0.07	7.2	80	408.0	0.035	26.6	9.3	32	35	247	1520
	Mean	28.8	65.0	6.2	1.02	0.04	5.5	43	129.7	0.026	17.8	6.8	21	25	97	789
	Median	27.0	66.8	5.7	1.02	0.04	5.8	46	68.6	0.028	19.0	6.9	20	25	78	638
003	Min	24.4	59.5	4.2	0.95	0.02	3.9	22	9.1	<0.01	12.4	4.3	17	20	31	610
	Max	36.4	69.2	7.0	1.90	0.11	6.3	40	77.0	0.072	19.4	11.0	27	35	67	897
	Mean	31.0	63.6	5.4	1.39	0.06	5.0	30	30.7	0.033	16.0	7.6	22	28	46	772
	Median	31.8	63.0	5.2	1.36	0.06	5.0	29	27.4	0.025	15.7	7.5	22	28	44	797
004	Min	39.0	51.2	3.5	0.49	0.02	2.9	18	8.9	<0.01	9.2	3.6	13	17	25	469
	Max	45.2	56.5	4.5	0.78	0.08	4.2	26	22.9	0.018	12.5	7.1	19	24	39	785
	Mean	41.6	54.5	3.9	0.58	0.04	3.6	21	13.1	0.014	11.1	4.9	15	19	29	593
	Median	41.9	54.5	3.8	0.54	0.05	3.7	20	11.1	0.015	11.0	4.6	15	18	28	576
005	Min	49.8	29.9	2.1	0.86	0.02	3.0	17	6.0	<0.01	9.4	2.5	13	13	24	520
	Max	67.9	45.4	5.0	1.56	0.09	4.0	26	17.4	0.020	13.6	7.3	19	32	39	685
	Mean	55.6	40.5	3.8	1.28	0.05	3.6	21	11.2	0.016	11.5	5.0	16	19	30	597
	Median	52.5	43.1	4.0	1.29	0.04	3.5	20	9.8	0.017	11.2	4.9	16	17	30	575
007	Min	54.4	35.6	2.6	0.45	0.02	3.2	16	7.6	<0.01	9.4	3.3	14	15	23	415
	Max	61.7	41.4	4.1	0.70	0.07	3.9	22	13.3	0.019	11.7	7.1	18	23	32	605
	Mean	58.1	38.3	3.6	0.55	0.04	3.5	19	10.7	0.014	10.5	5.4	16	19	27	493
	Median	58.0	38.3	3.8	0.56	0.04	3.5	18	11.3	0.013	10.5	6.0	16	18	27	481
008	Min	48.7	42.6	3.8	0.46	0.02	3.0	16	10.2	<0.01	9.9	4.6	12	16	22	357
	Max	53.6	46.8	4.5	0.66	0.03	3.7	20	14.7	0.013	11.3	5.8	15	20	30	453
	Mean	50.5	45.4	4.2	0.58	0.02	3.3	18	12.8	0.012	10.4	5.4	14	18	26	399
	Median	50.2	45.5	4.2	0.60	0.02	3.3	18	13.0	0.012	10.2	5.5	14	18	26	391
009	Min	22.1	56.4	4.7	0.82	0.06	3.0	17	6.6	<0.01	10.2	3.1	14	15	22	369
	Max	38.9	70.9	7.9	1.89	2.20	45.0	259	158.0	0.034	161.0	76.0	235	269	324	6340
	Mean	28.3	65.5	6.2	1.33	0.25	6.6	39	24.4	0.022	22.5	10.4	33	39	49	892
	Median	28.5	65.4	5.9	1.17	0.15	4.6	27	15.3	0.025	14.8	6.8	22	28	33	576

(Continued)

Table 4. Continuation.

Core-ID	Sand [vol. %]	Silt [vol. %]	Clay [vol. %]	TOC [wt. %]	As [mg/kg]	Cd [mg/kg]	Co [mg/kg]	Cr [mg/kg]	Cu [mg/kg]	Hg [mg/kg]	Ni [mg/kg]	Pb [mg/kg]	V [mg/kg]	Zn [mg/kg]	Ba [mg/kg]	Ti [mg/kg]
<i>010</i>																
Min	55.3	35.7	2.6	0.49	1.6	0.01	2.5	14	6.6	<0.01	8.2	3.4	13	15	21	343
Max	61.7	40.3	4.4	0.70	3.2	0.06	3.5	21	16.4	0.017	11.7	6.3	17	22	30	561
Mean	58.7	37.8	3.5	0.60	2.1	0.03	3.1	17	10.9	0.014	10.2	5.2	15	18	26	454
Median	57.9	38.4	3.8	0.65	1.8	0.02	3.1	17	11.1	0.015	10.5	5.5	15	18	26	470
<i>011</i>																
Min	65.9	22.4	2.2	1.35	1.6	0.02	2.7	13	4.6	<0.01	9.2	2.4	12	10	18	373
Max	75.4	30.3	4.1	1.73	4.3	0.09	3.7	21	11.4	0.017	12.3	6.6	19	21	37	904
Mean	70.0	27.0	3.0	1.53	2.7	0.05	3.3	17	7.5	0.015	10.5	3.9	15	14	26	547
Median	70.2	27.0	2.8	1.52	2.8	0.05	3.3	16	6.8	0.015	10.6	3.2	15	13	25	476
<i>013</i>																
Min	69.8	18.6	1.7	0.54	1.4	0.02	2.6	15	6.4	<0.01	8.1	3.0	11	12	16	324
Max	79.8	26.7	3.9	0.74	4.8	0.12	3.9	23	10.6	0.016	12.7	6.7	18	21	32	722
Mean	72.4	24.6	3.0	0.61	2.9	0.05	3.3	19	7.6	0.014	10.3	4.9	14	16	23	445
Median	71.8	25.4	2.9	0.59	2.8	0.04	3.3	20	7.6	0.014	10.0	5.4	14	16	23	375
<i>1039</i>																
Min	14.2	44.3	4.5	0.03	0.7	0.01	6.4	59	137.0	0.036	21.9	1.2	11	12	104	390
Max	51.2	77.3	9.2	1.08	4.7	0.05	9.3	140	326.0	0.071	35.1	7.1	25	32	183	861
Mean	23.7	69.2	7.0	0.52	2.8	0.02	7.9	102	237.6	0.052	29.4	4.1	18	22	132	617
Median	21.3	71.2	7.5	0.48	3.0	0.02	8.0	112	263.5	0.051	31.3	4.3	20	23	124	572
<i>1065</i>																
Min	5.9	30.5	3.5	0.31	0.6	0.00	2.4	18	8.8	-	8.9	3.4	14	12	26	-
Max	65.6	75.8	18.2	0.61	1.9	0.22	11.8	53	30.9	-	31.0	8.1	45	31	69	-
Mean	50.9	41.9	7.2	0.44	1.3	0.12	4.4	26	13.0	-	13.4	4.8	21	16	36	-
Median	59.8	35.2	4.6	0.43	1.4	0.13	2.9	21	9.9	-	10.2	4.7	16	14	30	-
<i>1075</i>																
Min	38.8	43.5	2.6	0.48	2.1	0.02	3.4	21	7.9	<0.01	10.6	3.3	17	16	32	747
Max	53.5	56.0	5.2	0.88	3.3	0.08	5.1	31	27.0	0.022	15.6	7.3	25	28	55	931
Mean	47.2	48.9	3.8	0.66	2.6	0.05	4.0	25	14.9	0.017	12.3	5.2	20	20	40	869
Median	48.0	48.3	3.7	0.63	2.6	0.05	3.9	25	12.5	0.018	12.1	5.0	20	20	39	871
<i>1079</i>																
Min	1.8	71.3	4.8	0.13	3.4	0.61	4.5	39	20.4	-	20.6	3.2	14	28	46	-
Max	23.8	85.4	13.0	1.72	9.1	0.86	9.2	147	1316.1	-	45.7	11.1	27	55	760	-
Mean	13.6	78.0	8.3	0.90	6.0	0.72	6.3	87	388.7	-	29.8	7.9	22	41	259	-
Median	15.6	77.4	7.8	1.10	6.2	0.71	5.8	66	175.0	-	25.8	9.0	25	40	115	-
<i>1087</i>																
Min	20.2	43.2	4.1	0.40	3.4	0.43	2.9	23	13.9	-	12.4	3.5	17	28	30	-
Max	52.7	66.3	13.5	1.19	5.7	1.09	8.4	46	29.7	-	24.3	6.7	35	50	62	-
Mean	43.5	50.4	6.1	0.80	4.6	0.64	4.5	31	19.7	-	16.1	5.3	23	38	42	-
Median	46.4	48.9	4.9	0.86	4.7	0.56	3.6	28	18.8	-	14.2	5.3	21	36	38	-
<i>1089</i>																
Min	15.4	66.7	4.2	0.76	3.4	0.02	5.7	30	14.1	<0.01	16.2	6.8	24	29	49	986
Max	28.9	77.0	8.6	1.32	7.1	0.09	8.3	81	326.0	0.031	28.8	9.9	33	36	192	1230
Mean	22.2	72.2	5.6	0.99	4.6	0.05	4.7	47	94.0	0.023	20.2	8.3	28	32	89	1106
Median	22.2	72.4	5.4	0.93	4.1	0.05	6.6	46	69.4	0.025	20.2	8.4	28	31	85	1110

Table 5. Pearson's correlation matrix for heavy metals (As, Ba, Cd, Co, Cr, Cu, Hg, Ni, Pb, Ti, V and Zn) in all investigated samples (for location see Figure 1). Correlation coefficient (r) values are given in the lower triangle of the matrix, where $r > 0.7$ are highlighted in grey shading. Two-tailed probabilities (p) are given in the upper triangle of the matrix with $p > 0.05$, regarded as of low statistical significance, highlighted in grey writing.

	As	Ba	Co	Cr	Cu	Hg	Ni	Pb	V	Zn	Ba	Ti
As		0.03	0.00	0.00	0.11	0.91	0.11	0.02	0.00	0.00	0.00	0.00
Ba	0.13		0.00	0.00	0.00	0.00	0.00	0.00	0.00	0.00	0.00	0.00
Cd	0.19	-0.32		0.01	0.00	0.00	0.00	0.00	0.00	0.96	0.25	0.01
Co	0.19	0.83	-0.16		0.00	0.00	0.00	0.00	0.00	0.00	0.00	0.00
Cr	0.10	0.87	-0.32	0.89		0.00	0.00	0.00	0.00	0.00	0.00	0.00
Cu	0.01	0.85	-0.38	0.79	0.83		0.00	0.00	0.00	0.00	0.00	0.00
Hg	-0.13	0.26	-0.32	0.25	0.28	0.33		0.00	0.00	0.08	0.00	0.00
Ni	0.14	0.84	-0.21	0.94	0.92	0.82	0.26		0.00	0.00	0.00	0.00
Pb	0.23	0.45	-0.30	0.42	0.42	0.51	0.34	0.42		0.00	0.00	0.00
Ti	0.23	0.40	0.00	0.43	0.40	0.20	0.15	0.36	0.46		0.00	0.00
V	0.42	0.56	-0.07	0.64	0.58	0.46	0.23	0.59	0.74	0.74		0.00
Zn	0.26	0.52	-0.16	0.55	0.53	0.50	0.27	0.57	0.83	0.57	0.84	

Table 6. Sediment accumulation rates (SARs) estimated for eight cores (for location see Figure 1). For details see section 3.4 and 4.3.

Core-ID	Intervals used for ^{210}Pb -derived SARs estimation [cm depth]	Sediment accumulation rate [mm yr ⁻¹]	
		^{210}Pb (min – max)	^{137}Cs
001	2 – 5	~1.5 (1.3 – 1.6)	>1.1
002	2 – 4	1.9 (0.6 – 2.0)	>2.9
	3 – 12	2.5 (2.1 – 2.6)	
	12 – 17	2.1 (1.4 – 2.6)	
003	5 – 12	1.1 (0.8 – 1.2)	1.4
005	5 – 11	1.5 (1.1 – 1.8)	1.3
013	5 – 9	0.7 (0.4 – 0.8)	1.2
1065	2 – 6	0.9 (0.7 – 1.1)	1.5
1075	2 – 8	0.9 (0.6 – 1.1)	0.8
1079	2 – 5	1.2 (1.2 – 1.3)	>2.7
	4 – 16	4.3 (3.7 – 4.7)	
	15 – 20	3.6 (2.7 – 4.1)	

Table 7. The Norwegian environmental quality classification of metal contaminants in marine sediments (Bakke et al., 2010 after SFT, 2007).

	I Background	II Good	III Moderate	IV Bad	V Very bad
	Background levels	No toxic effects	Toxic effects following chronic exposure	Toxic effects following short-term exposure	Severe acute toxic effects
As [mg/kg]	<20	20 – 52	52 – 76	76 – 580	>580
Cd [mg/kg]	<0.25	0.25 – 2.6	2.6 – 15	15 – 140	>140
Cr [mg/kg]	<70	70 – 560	560 – 5900	5900 – 59000	>59000
Cu [mg/kg]	<35	35 – 51	51 – 55	55 – 220	>220
Hg [mg/kg]	<0.15	0.15 – 0.63	0.63 – 0.86	0.86 – 2	>2
Ni [mg/kg]	<30	30 – 46	46 – 120	120 – 840	>840
Pb [mg/kg]	<30	30 – 83	83 – 100	100 – 720	>720
Zn [mg/kg]	<150	150 – 360	360 – 590	590 – 4500	>4500

Figure 1. Location map with study area marked by black rectangles in A) regional and B) local context. Crossed hammers in B indicate the location of Ulveryggen mine. C) Map of Repparfjorden showing the locations of coring stations (for details see Table 1). Black circles on C indicate sediment cores for which results are presented within this manuscript; results for cores reflected with black circles/white fill are provided in Supplementary Figure 1 and 2. Green star indicates location of sediment core SED kjerne from Christensen et al. (2011). Dashed line marks a sill that separates inner from outer fjord. Red arrow indicates the probable position of pipeline outlet through which mine tilings were discharged in the 1970's.

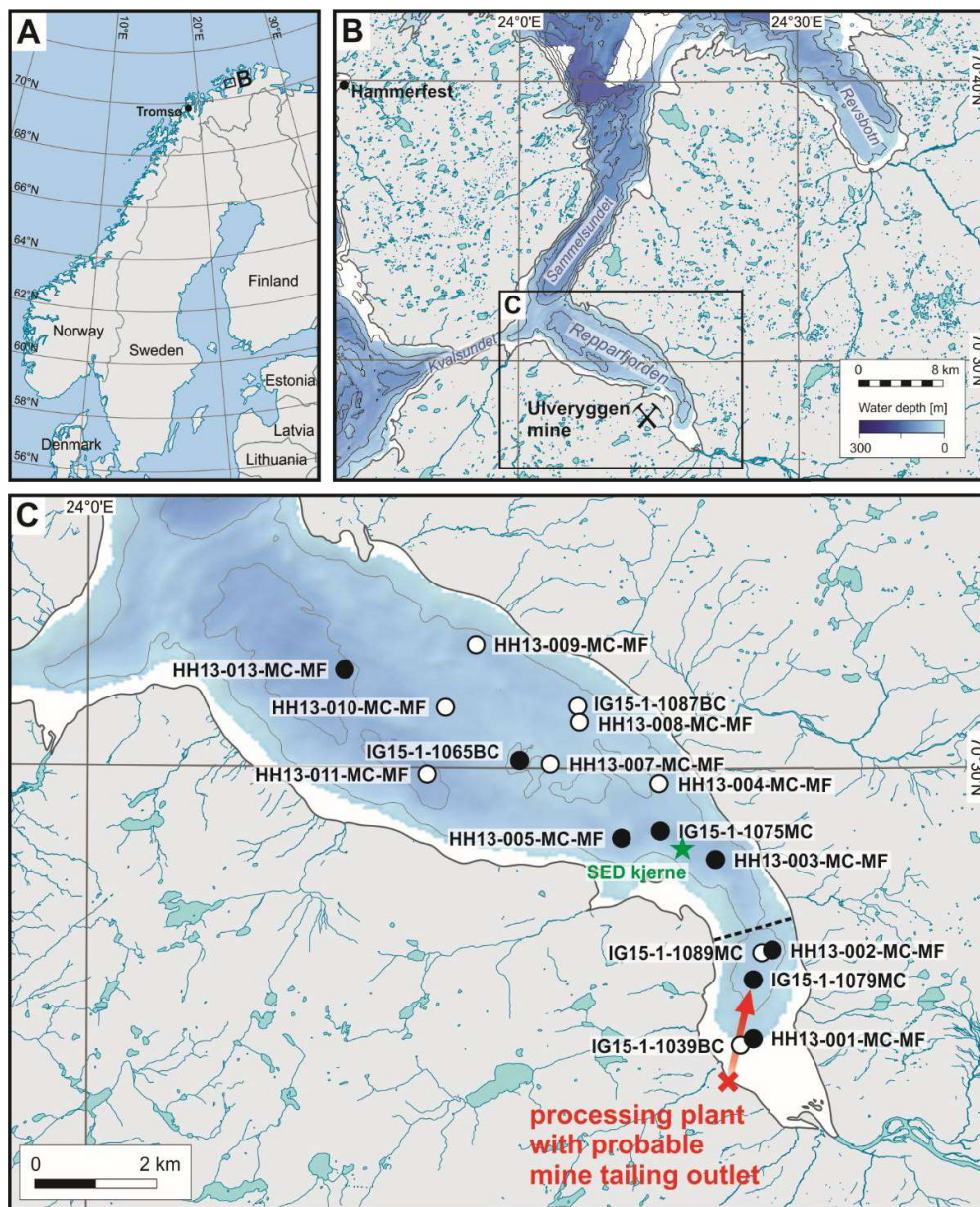
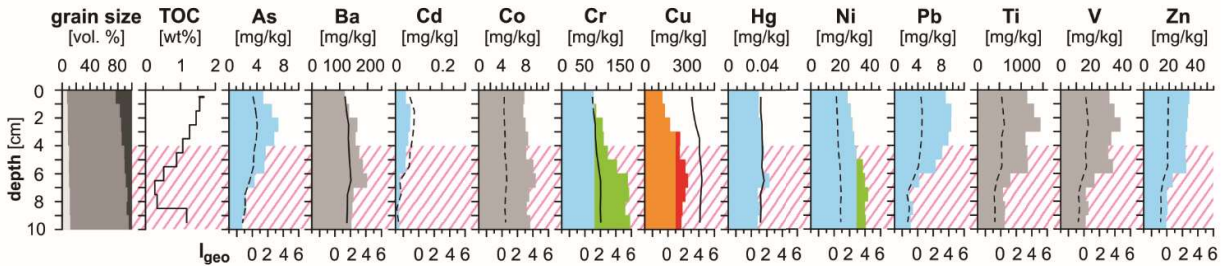
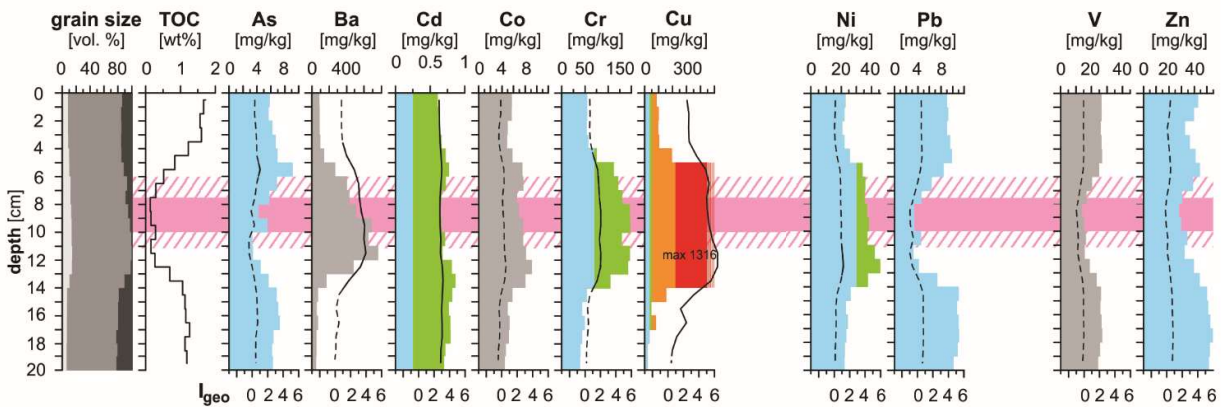


Figure 2. Sedimentological and geochemical properties versus depth of eight sediment cores (for locations see Figure 1 and Table 1). Grain-size composition (clay – light, silt – medium and sand – dark grey). Total organic carbon (TOC) content. Heavy metal (As, Ba, Cd, Co, Cr, Cu, Hg, Ni, Pb, Ti, V and Zn) concentrations (upper x-axis); the color scale is in line with the Norwegian marine sediment quality classification of contaminants in marine sediments (see Table 7) (SFT 2007) (gray color is applied for metal concentrations not included in this classification); calculated values of geoaccumulation index (I_{geo}) after Müller (1969) where values of classes 0-1 are shown as dotted lines and classes >1 as solid lines. Pink horizontal bars mark the period of mine tailing disposal (1972-1978) based on the ^{210}Pb -derived and recalculated sediment accumulation rates (SARs) whereas the pink shading represents maximum and minimum ^{210}Pb - and ^{137}Cs -derived SARs (see Table 5).

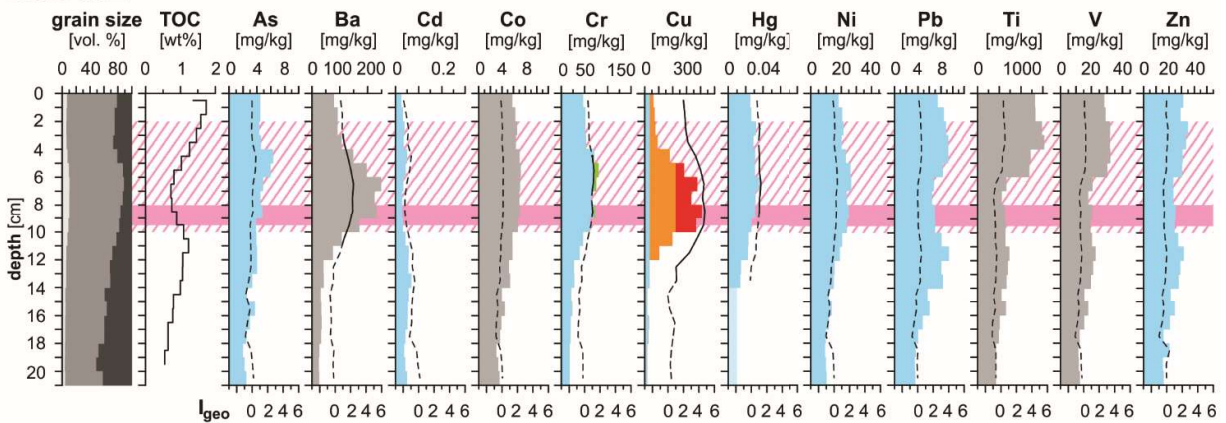
core 001



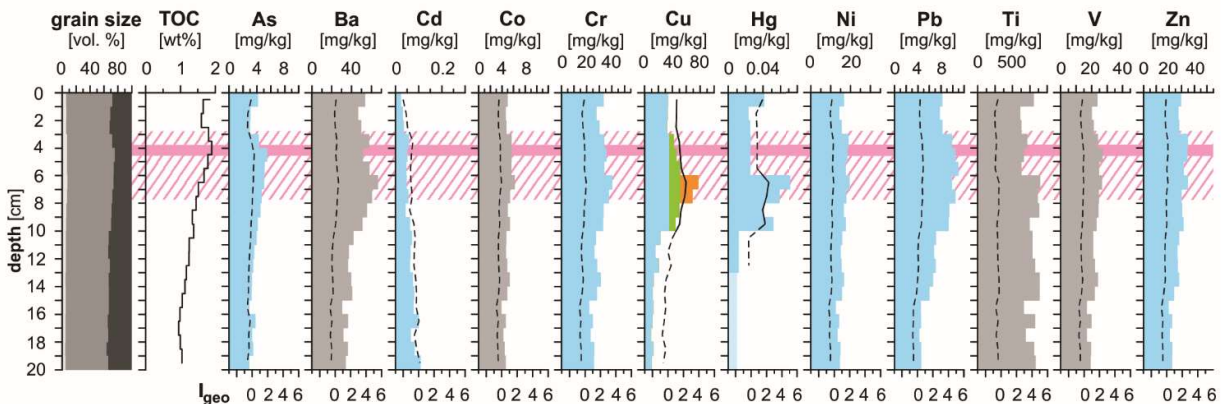
core 1079



core 002

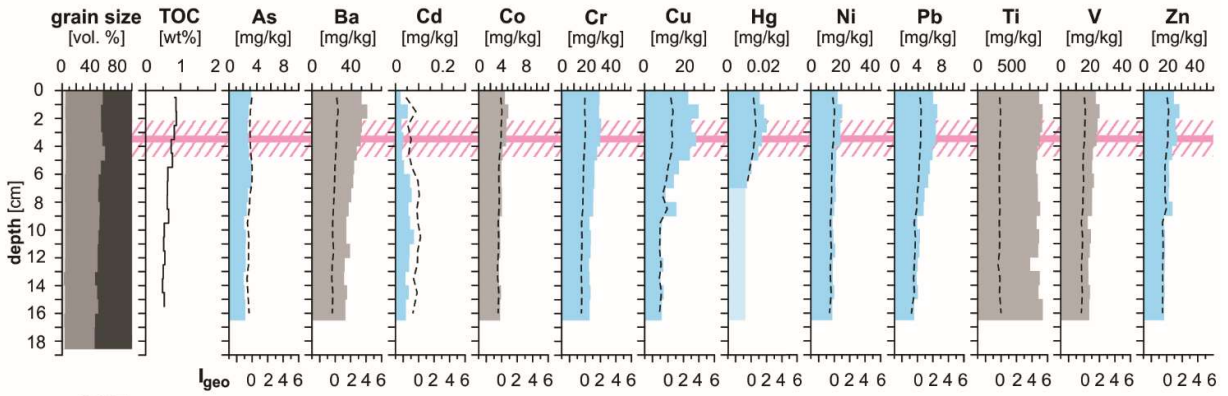


core 003

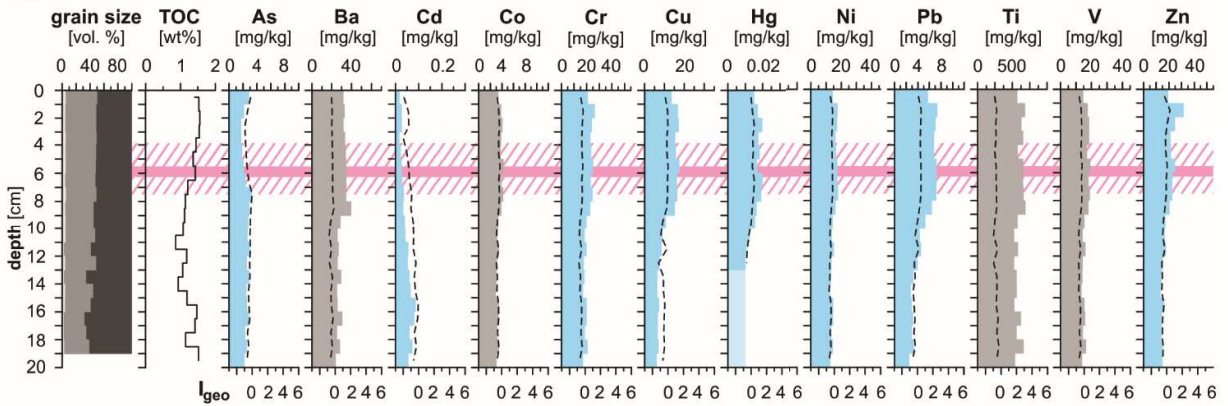


Continuation of Figure 2.

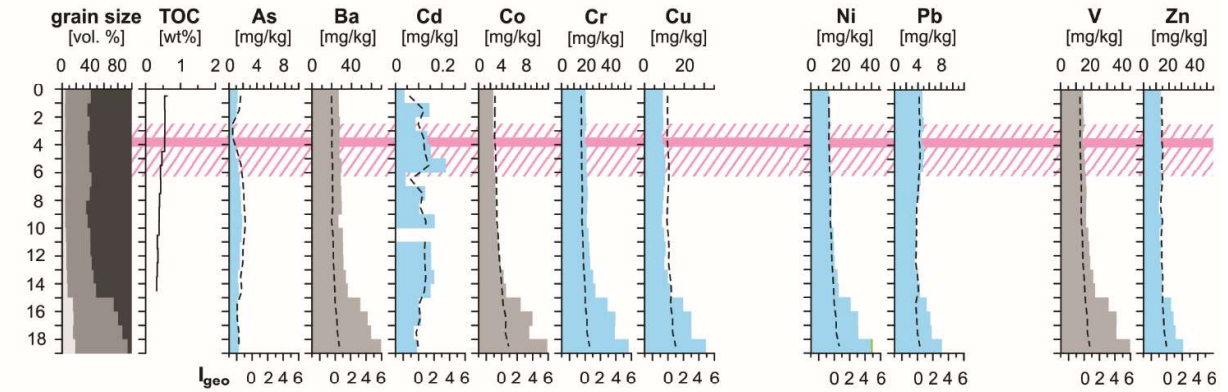
core 1075



core 005



core 1065



core 013

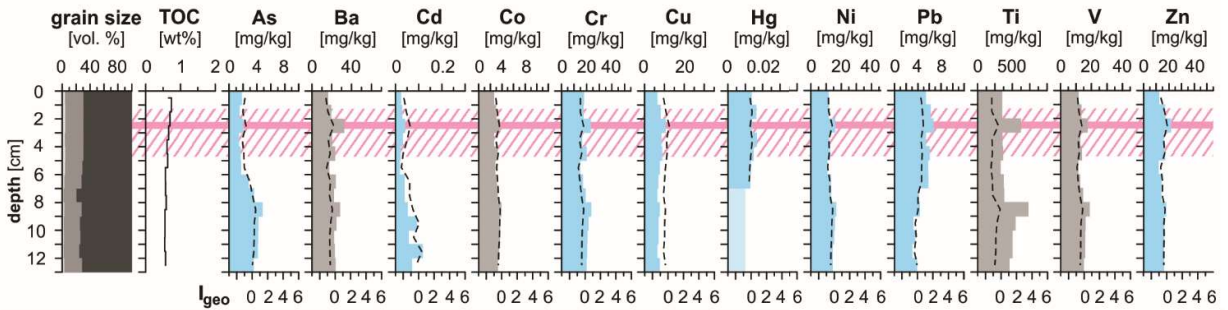


Figure 3. Textural classification of all analyzed samples from all sediment cores (bottom panel) presented as sand-silt-clay triangular diagram (after Folk 1954). Cores taken from different parts of Repparfjorden are marked by the following symbols color: white – inner fjord, light grey – northeastern part of outer fjord and dark grey – southwestern part of outer fjord.

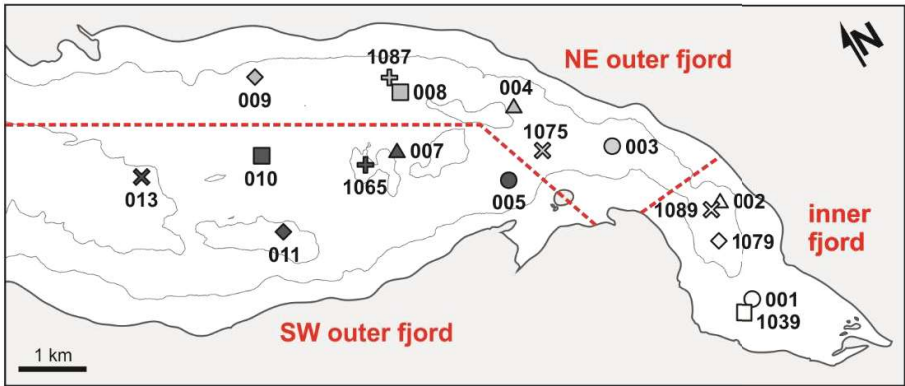
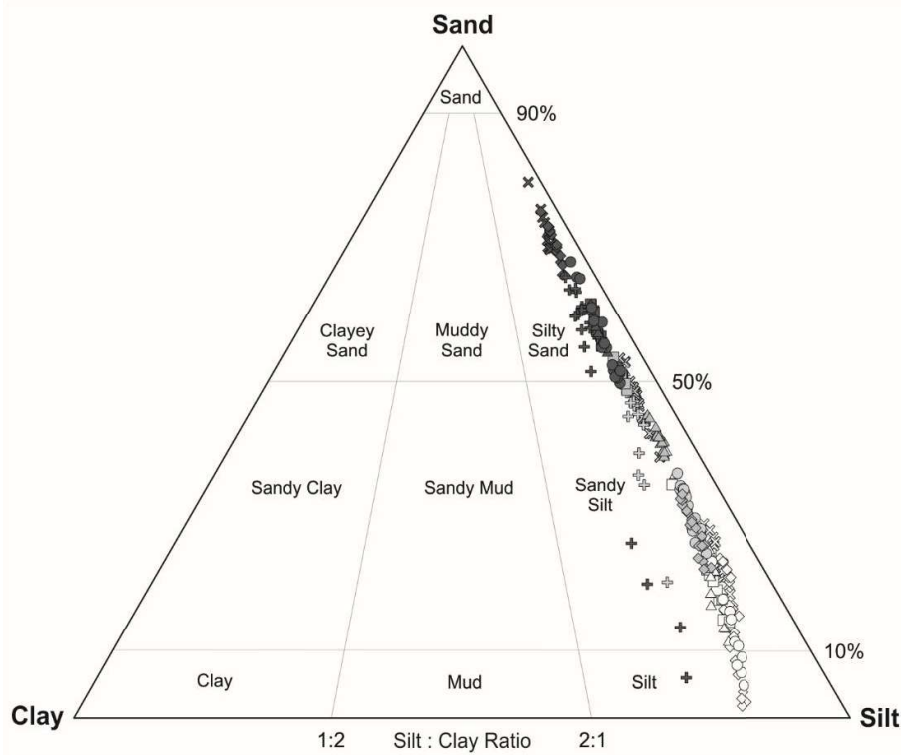


Figure 4. Frequency curves of grain-size distributions of eight selected sediment cores (for location see Figure 1 and Table 1).

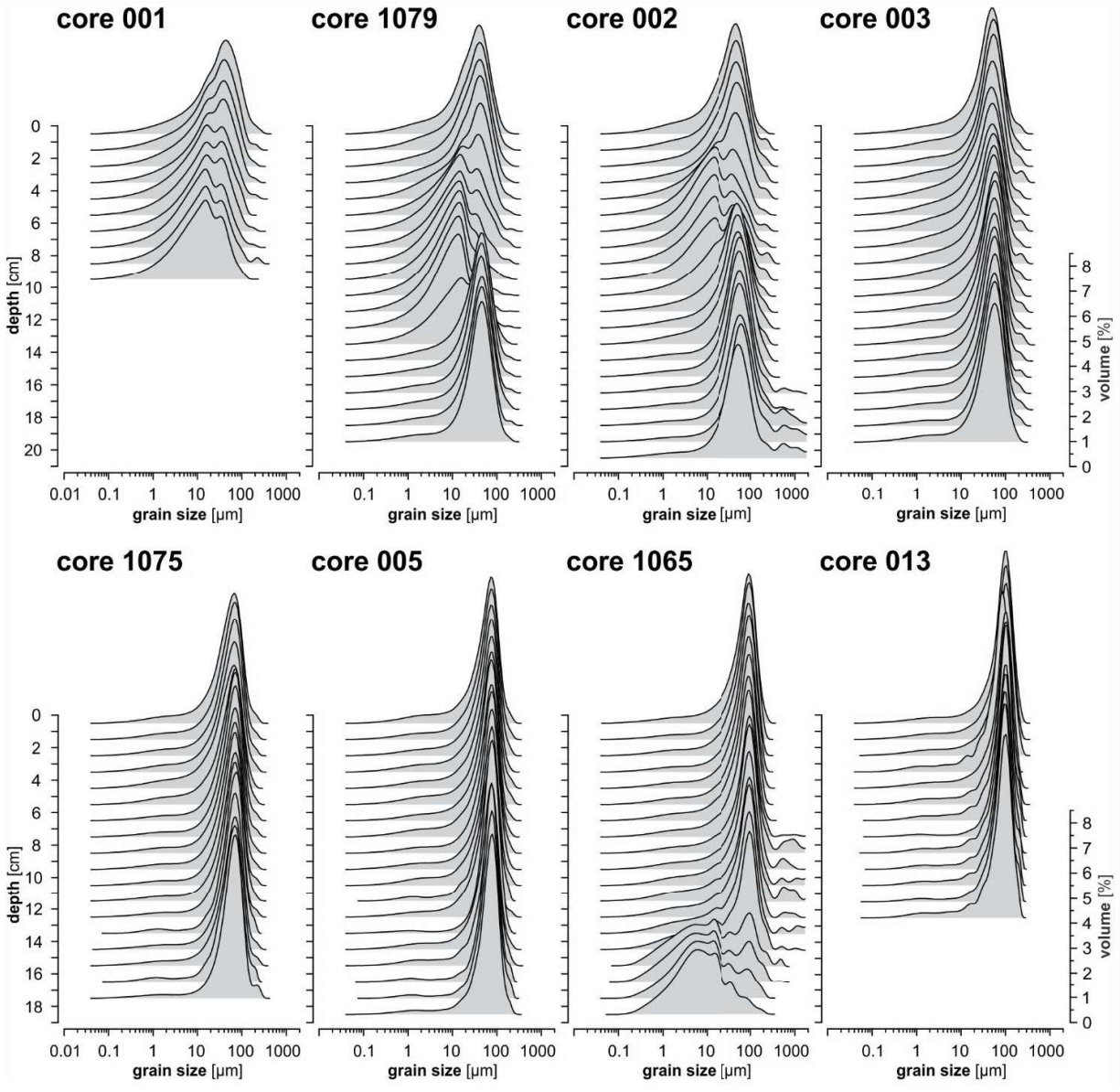


Figure 5. ^{210}Pb (upper x-axis) and ^{137}Cs (lower x-axis) activity profiles of eight selected sediment cores (for location see Figure 1 and Table 1). The horizontal error bars mark the 2-sigma measurement uncertainties.

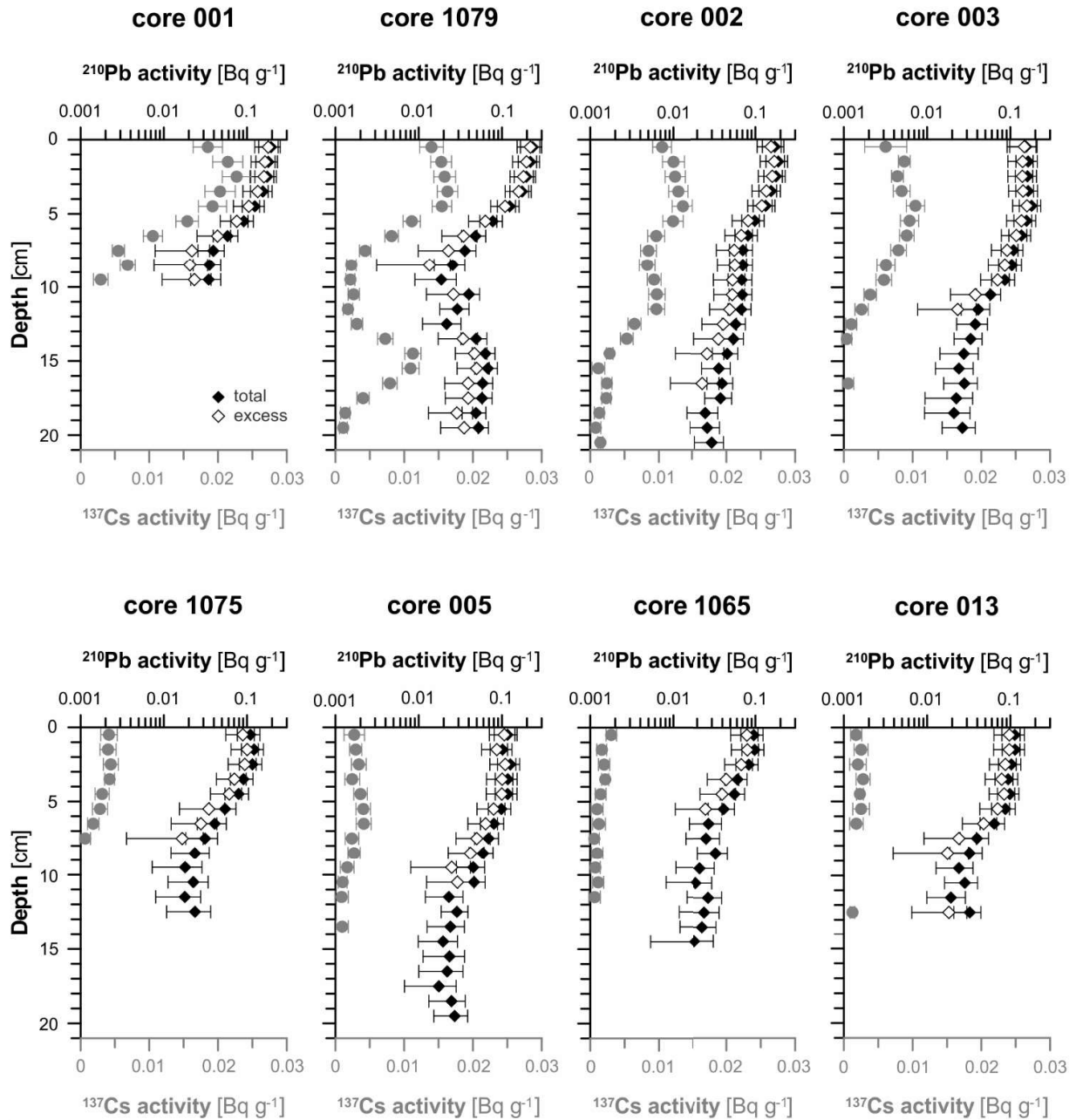
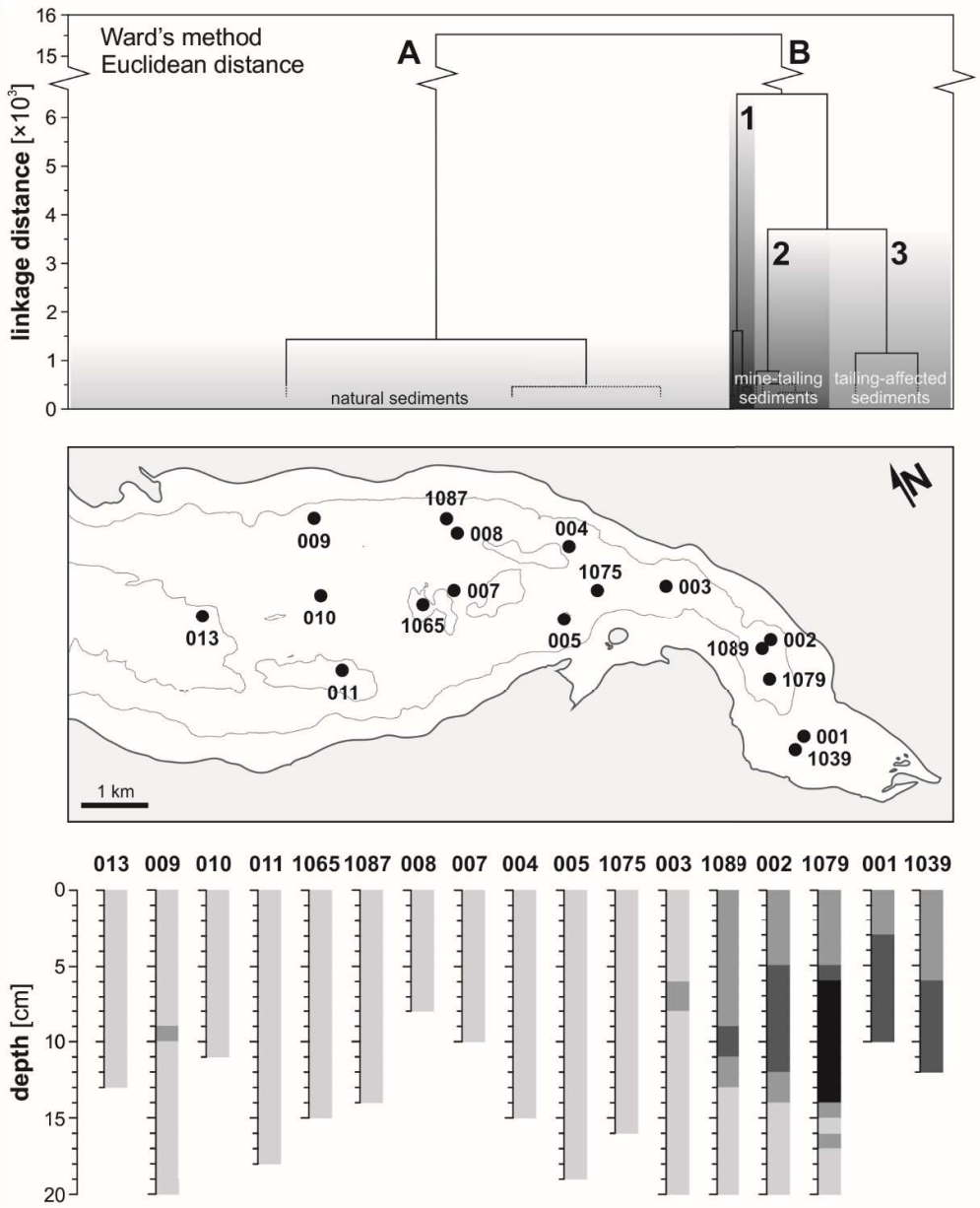


Figure 6. Cluster analysis of 261 sediment samples of all investigated cores based on their sedimentological and geochemical signatures (for details see section 5.1). The smaller the linkage distance the bigger similarity between the samples. Distinguished clusters and sub-clusters (*A*, *B1*, *B2* and *B3*) marked in gray shading (top and bottom panel) refer to sediment types discussed in the main text.



Supplementary Data

[Click here to download Supplementary Data: Sternal et al_SupplementaryTables.docx](#)

Supplementary Data

[Click here to download Supplementary Data: Sternal et al_SupplementaryFigures.docx](#)